Synthesis and characterization of bimetallic metal oxide on graphene support electrocatalyst for carbon dioxide conversion

Thesis
Submitted in partial fulfillment for the award of degree
of

Master of Science in Chemistry

By

GAGANDEEP KAUR
(Registration No.: 301602020)

Under the guidance of

Dr. Haripada Bhunia
Professor & Head
Department of Chemical Engineering

Dr. Davinder Kumar
Assistant Professor
School of Chemistry and Biochemistry

SCHOOL OF CHEMISTRY AND BIOCHEMISTRY

THAPAR INSTITUTE OF ENGINEERING AND TECHNOLOGY,

PATIALA-147004, PUNJAB

CERTIFICATE

This is to certify that the dissertation entitled **"Synthesis and characterization of bimetallic metal oxide on graphene support electrocatalyst for carbon dioxide conversion"** being submitted by Ms. Gagandeep Kaur to School of Chemistry and Biochemistry, Thapar Institute of Engineering and Technology, Patiala in partial fulfillment of the requirements for the award of degree of **Master of Science in Chemistry,** is an authentic record of bonafide work carried out by her under our guidance and supervision. She has fulfilled the requirements for the submission of this thesis, which to our knowledge has reached the requisite standard.

The results embodied in the thesis have not been submitted in part or full to any other University or Institute for the award of any degree or diploma.

3/8/18

(Dr. Haripada Bhunia)
Professor & Head
Department of Chemical Engineering

Davinder Kumar

(Dr. Davinder Kumar)
Assistant Professor
School of Chemistry and Biochemistry

ACKNOWLEDGEMENT

Today, when I look back into my life, it feels that no road is too tough to be walked on. With the guidance and encouragement of elders, and hard work; impossible can also be turned into possible. It was nearly impossible to accomplish my project without the help and inspiration extended by these personalities and I would not forget to thank them.

Although it is difficult to translate the feelings of regards into reality, yet it is detectable when I execute my sense of profound respect to my supervisors **Dr. Haripada Bhunia**, Department of Chemical Engineering and **Dr. Davinder Kumar**, School of Chemistry and Biochemistry, for their guidance, thoughtful planning, knowledge and motivation during the course of my project. I respect him for inspiring me in many ways and it's been a great honour to work under their guidance.

I am also grateful to **Dr. Neetu Singh**, Department of Chemical Engineering for advising and guiding me towards right direction. I am deeply thankful to **Dr. Amjad Ali**, Head, School of Chemistry and Biochemistry for offering me the opportunity to explore the research work and allowing me to use various facilities in respective departments.

I would like to thank my lab research scholars **Mr. Jaswinder Singh, Mr. Mohit Kumar, Mr. Dev Mandal, Mr. Sunil Sable and Mr. Saudagar Dongre** and for sharing their experiences and helping in lab activities which helped a lot in understanding the work well. I also want to thank my friend **Ms. Arshdeep Kaur** for helping me whenever I required.

I express my deepest gratitude to my parents for their blessings, endless love, support, encouragement. Without them, this journey would not be completed. I would like to dedicate my achievement to them.

Above all, I express my indebtedness to **Almighty God** whose blessings and kindness helped to complete this work successfully.

Gagandeep Kaur

ABSTRACT

The furthermost challenge of twenty-first century is increasing amount of green house gas, Carbon dioxide (CO_2), in the atmosphere due to fossil-fuels and energy-demanding industries. The concerns of problems like global warming and climate change has led to initiate global efforts to reduce the emission and concentration of CO_2. Replacement of fossil fuels with renewable energy sources, to reduce CO_2 emission is considered from past years. Due to the increase in atmospheric temperature, this problem has attracted the attention of scientific community globally. Carbon dioxide capture and sequestration (CCS) technology has appeared as a first solution to this problem and has gained higher interest, as it could decrease the amount of CO_2 into atmosphere. However, higher energy consumption and the risk of leakage of stored CO_2 in this process, prevents its large scale up development. Instead of CO_2 capture and sequestration its utilization to produce useful chemicals is a better solution. This approach not only provides fuels and useful chemicals but also helps in reducing the amount of CO_2 in the atmosphere and cost of CCS process.

Many techniques are available for CO_2 reduction, such as photochemical, radiochemical, biochemical, electrochemical and thermochemical reduction. The reduction of CO_2 becomes a challenging task due to its highly stable nature. Out of all available techniques, electrochemical reduction is believed to be best owing to its advantages, such as controllable electrode potential, reaction temperature, production of alcohols, and hydrocarbons from renewable energy sources and easy for scale up applications. Numerous challenges are associated with the electrochemical reduction of CO_2, i.e. occurrence of hydrogen evolution reaction (HER) and formation of multiple products. It is essential/desirable to develop an appropriate electrocatalyst which can produce chemicals selectively with high faradic efficiency and should be durable.

Copper based electrocatalysts are found to be attractive and have been extensively used for electrochemical reduction of CO_2 due to its unique capability to catalyze the formation of hydrocarbons. Many researchers have performed their work by modifying copper electrode and found interesting results. In this work, graphene supported bi-metallic metal oxide electrocatalyst (Cu_2O-ZnO) was synthesized for its use in electrochemical reduction to convert CO_2 to chemicals/fuels. The synthesized electrocatalyst were characterized using various techniques namely XRD (X-ray diffraction), XPS (X-ray photoelectron spectroscopy), Raman spectroscopy and FE-SEM (Field emission scanning electron microscopy). On the basis of characterization results, prepared electrocatalyst is found suitable to be used for electrochemical reduction of CO_2 to fuels/chemicals.

Keywords: Carbon dioxide, electrocatalyst, electrochemical reduction, fuel, graphene oxide.

THESIS OVERVIEW

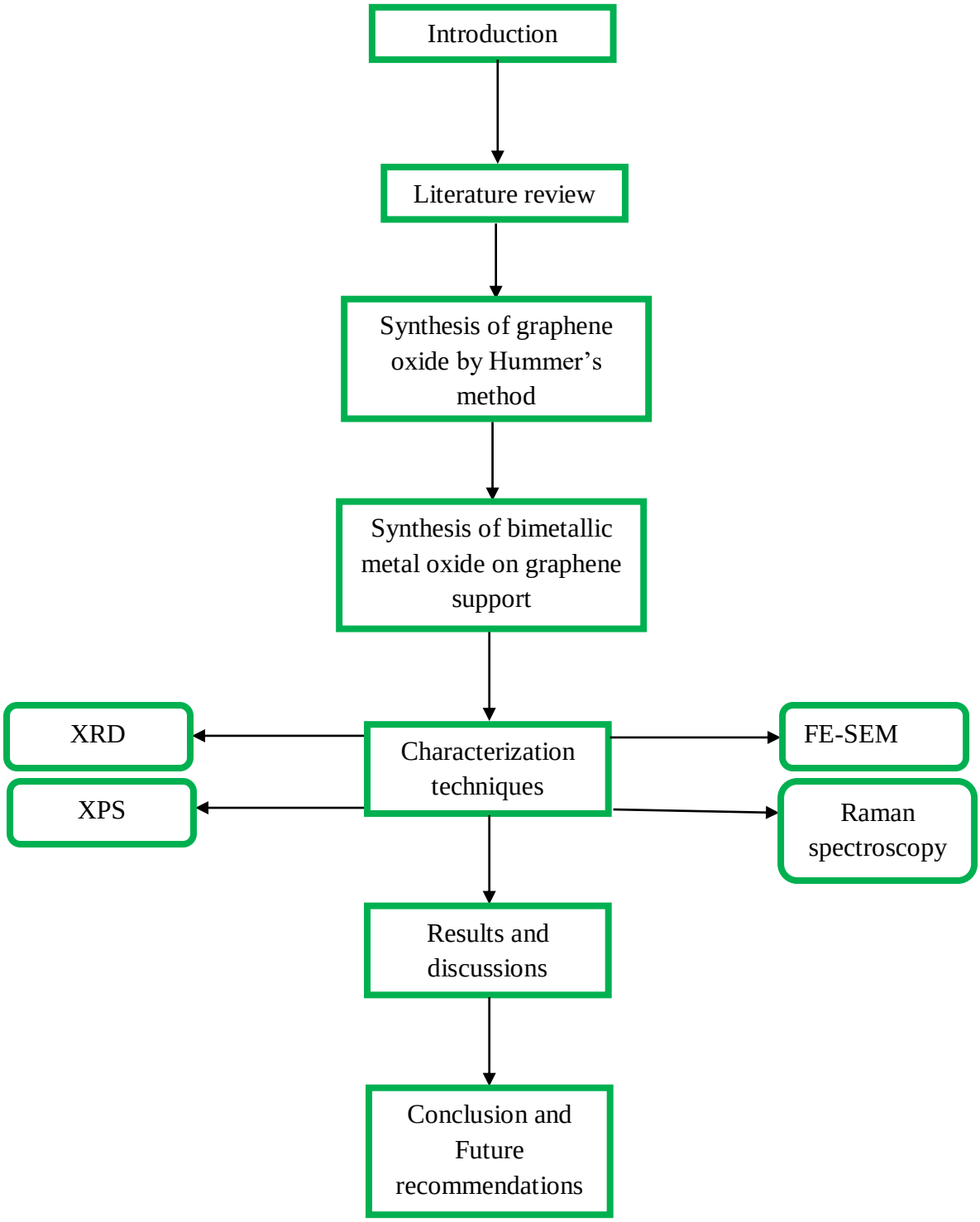

TABLE OF CONTENTS

LIST OF TABLES

LIST OF FIGURES

LIST OF SYMBOLS AND ABBREVIATIONS

SYMBOLS

Å	Angstrom
B	Full width at half maximum
°C	Degree Celsius
E°	Electrode potential
F	Faraday's constant
k	Constant representing shape
n	Number of moles
t	Crystal thickness
V	Volt
Q	Total charge passed

ABBREVIATIONS

B.E.	Binding energy
CO_2	Carbon dioxide
Cu_2O	Cuprous oxide
$CuCl_2$	Copper chloride
ERC	Electrochemical reduction of carbon dioxide
FE	Faradaic efficiency
FE-SEM	Field emission scanning electron microscopy
FWHM	Full width at half maximum
GN	Graphene
GO	Graphene oxide

H_2O_2	Hydrogen peroxide
H_2SO_4	Sulphuric acid
IPCC	Intergovernmental Panel on Climate Change
NaOH	Sodium hydroxide
$NaNO_3$	Sodium nitrate
$NH_4OH.HCl$	Hydroxyl ammonium chloride
ppm	Parts per million
RHE	Reversible hydrogen electrode
XRD	X-ray diffraction
XPS	X-ray photoelectron spectroscopy
$ZnCl_2$	Zinc chloride

Greek Letters

α	Amount of electrons passed
θ_B	Bragg's angle
η	Overpotential

CHAPTER 1 – INTRODUCTION

The two major issues of the world- depletion of fossil fuels and the increasing concentration of CO_2, which are unavoidable, have been discussed in this chapter. The details of present state of environment and various approaches such as carbon capture and sequestration (CCS) and CO_2 utilization are also discussed. Along with that, this chapter also detailed out the advantages of electrochemical reduction of CO_2 in dealing with existing environment problems and the challenges encountered in this field.

1.1 Background

In the world of increasing fossil fuel usage, it has to deal with major energy related issues in next 50 years. Firstly, consumption of fossil fuel reserves increased worldwide competition which will lead to rise in costs. Secondly, increasing in concentration of atmospheric CO_2 will cause the drastic change in environment which is very harmful (climate change). Carbon is primarily source of not only living beings but also a part of air, oceans i.e. atmosphere and hydrosphere respectively. Carbon present in atmosphere in combination with oxygen as carbon-dioxide. To avoid unwanted climate changes there is a need to control increasing atmospheric levels of CO_2. Carbon dioxide, a linear molecule having bond distance C-O of 1.16 Å. Overall, it is a non-polar but due to difference in electronegativity of carbon and oxygen, it contains polar bonds too. Due to its non-basic nature, it interacts with Bronsted and Lewis acids very weakly. It sticks in atmosphere longer than other greenhouse gases so considered as an important long lived gas. The presence of CO_2 is approximately 0.03% but it possesses huge impact on living organisms.

The increase in level of CO_2 is related to rise in global warming. The payback of this issue would be more then droughts, disasters. Scientists believed that due to overconsumption of fossil fuels, global temperature continues to rise. There is a need to reduce CO_2 to overcome the undesirable effects of global warming and climate changes. In the process of photosynthesis, plants taken up the carbon-dioxide. All respiring organisms, volcanic emissions are natural source of CO_2 in atmosphere. Thus, inflow and outflow of CO_2 remains maintained and this natural flow through various spheres are known as carbon cycle. In order to expel a fossil feedstock, closing the carbon cycle by utilization of CO_2 as a feedstock is a relevant intermediate step towards carbon free world. However, if there is more inflow of CO_2 increases the carbon balance. According to recent researches, safe level of CO_2 for human civilization is 350 ppm[1]. Due to increase in industrialization, fossil fuel emissions,

deforestation etc., CO_2 level rises up. The other source which also harms the environment is increasing use of transportation. It is considered in fastest rising source of CO_2 emission and according to Energy Technology Perspectives the emission will be double by 2050 (IEA 2010). The increased use of vehicles leads to depletion of conservative fossil fuels. Dependency on fossil fuels results in change in climate and their depletion which needs to be solved.

1.2 CO_2 level in atmosphere

Industrialization and the usage of energy increased when human civilization took a leap in the beginning of 18^{th} century. In 1985, concentration of CO_2 in atmosphere crossed the safety barrier due to growing use of industrial processes and fossil fuels. Scientists made the speculations that the increasing trend of CO_2 will continue to rise. Therefore, some preventive measurements are necessary to reduce the increasing concentration of carbon dioxide.

To diminish the anthropogenic emissions of CO_2, Intergovernmental Panel on Climate Change (IPCC), set various types of targets. According to their report, in the last 250 years carbon dioxide concentration has worldwide grown by more than 100 ppm: from 275-285 ppm in the pre-industrial age to around 407.6 ppm in 2017 and it may continue to raise upto 570 ppm by 2100. Dependence on fossil fuels for requirement of energy leads to get higher in global temperature causing melting of glaciers, rise in level of sea[2]. Global sea level has risen by 0.19 m during 1901-2010. With the increase in CO_2 concentration in oceans which further increases the acidity due to pH drop by 0.1, marine life affected[3,4]. This continuous rise in the CO_2 level will cause the increase in global temperature by 2-6 °C, therefore CO_2 concentration stabilization to a level of 450 ppm is considered[5]. Figure 1.1 shows the amount of various gases which are responsible for greenhouse gas emissions (IPCC 2014)[6].

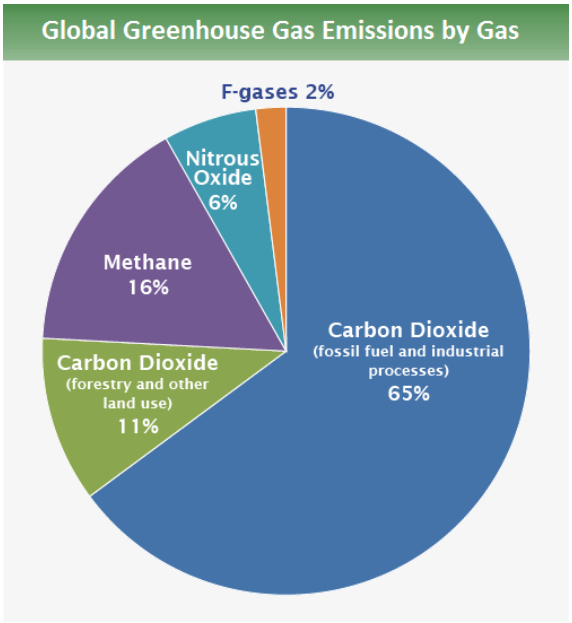

Fig. 1.1 Pie chart showing percentage of global greenhouse gas emissions [6]

1.3 Approaches to diminish global climate change

CO_2 emission and huge use of limited resources are sides of same coin and should be resolved together. There are different possible ways to deal with this issue:

- To switch from fossil fuel consumption to renewable resources such as solar, wind; however due to their periodic nature fraction of energy produced is only 30%.
- By capturing it and dump in oceans.
- By applying geo-engineering methods i.e. reforestation and afforestation.
- By converting it to either liquid fuels or useful economic products, which results in following improvement factors:
  - Minimizing its contribution towards greenhouse effect or global warming.
  - Reducing over dependency on fossil fuels, thus increasing energy security[7,8].

1.3.1 Carbon dioxide capture and sequestration (CCS)

To reduce the concentration of CO_2 and usage of fossil fuels for fulfill the energy needs, CCS is considered as key technology. There are various factors such as fuel cost, distance between capture and storage place etc. need to be considered related to cost for application of CCS on fossil fuels[3]. The choice of suitable CO_2 removal process is directly affected by the type of combustion process because CO_2 is produced during combustion.

There are different types of approaches through which CO_2 can be captured. These are – post-combustion, pre-combustion and oxy-combustion. CO_2 is capture previous to combustion in pre-combustion process, from flue gases produced during fuel burning with oxygen in place of ambient air in case of oxy-combustion and after combustion CO_2 is removed from flue gas in post-combustion method. Amongst them, the essential advantage is shown by post combustion process because it is well-suited to retrofitted combustion technologies without radical changes[8]. Figure 1.2 shows the schematic diagram for different CO_2 capture methods.

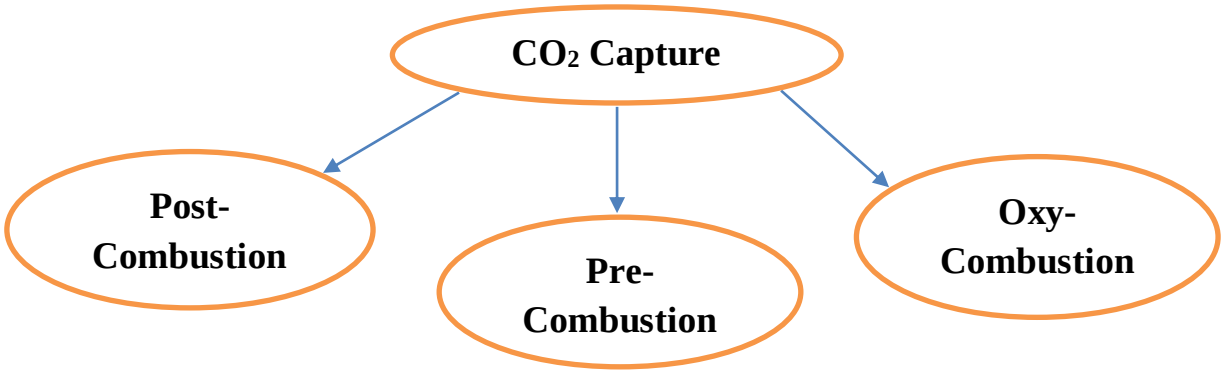

Fig. 1.2 Schematic diagram for different CO_2 capture methods

This process is cost and energy- consuming, and the major concerned related to it is the threat of leakage of stored CO_2, preventing the expansion of CCS[9]. Instead of CO_2 capture and sequestration its utilization to produce useful chemicals is a better solution.

1.3.2 CO_2 utilization

Due to increasing energy demands and decreasing fossil fuels, the most appropriate solution is CO_2 conversion into liquid fuels. It was used as feedstock a long ago for its conversion to various industrial products. It can be utilized as a solvent, in heat transfer and for synthesizing chemicals like formate and urea. To improve the atmosphere of greenhouse; carbon dioxide can be used for boosting of plant growth. The flue gases coming from the power plants i.e. carbon dioxide directly fixed with the help of microalgae. Various cyanobacteria lodge also in wastewater, reducing the fresh water and nutrient utilization and lowering the equipped cost. At last, biochemical processes such as manufacturing of succinic acid incorporate carbon dioxide.

The use of CO_2 as a feedstock does not mean it always generate eco-friendly and sustainable processes. There are some limitations such as consumption of fossil fuels for the synthesis of co-reactive materials such as epoxides, need of insufficient resources such as renewable energy sources, pipelines for catalysts, for the generation of hydrogen and

irrigation during biomass; lots of water is consumed and the utilization of energy, need to be taken into account[10].

1.4 CO_2 reduction

In recent years, CO_2 can be reduced by many ways such as photochemical, biochemical, radiochemical, electrochemical and thermochemical reduction. Figure 1.3 shows the schematic diagram of different ways of CO_2 reduction methods.

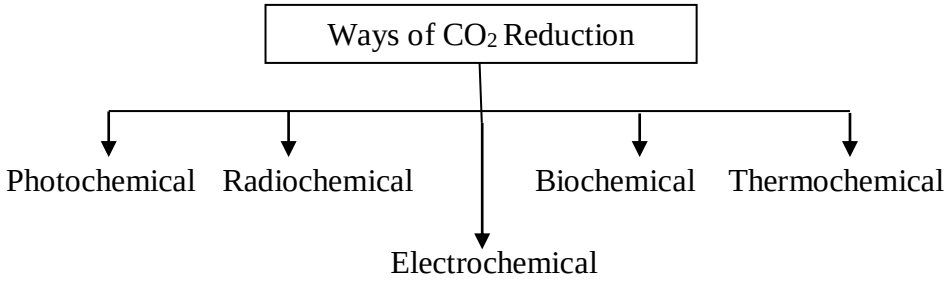

Fig. 1.3 Schematic diagram for different ways of CO_2 reduction methods

Out of them, electrochemical method is becoming most popular owing to its advantages.

- Production of value added or useful products like alcohols, hydrocarbons etc. Table 1.1 shows the list of various products formed during electrochemical reduction of CO_2
- Occurrence of reactions at room temperature.
- For a proton source, water can be used.
- Easy to handle.
- Free from harmful emissions.
- Formation of products with the help of renewable energy.

Table 1.1 List of various products formed during electrochemical reduction of CO_2[11]

Name of product & formula	Chemical reaction	E° (V versus RHE)
Ethylene (C_2H_4)	$2CO_2 + 12H^+ + 12e^- \longrightarrow C_2H_4 + 4H_2O$	0.08
Methane (CH_4)	$CO_2 + 8H^+ + 8e^- \longrightarrow CH_4 + 2H_2O$	0.17
Formaldehyde (HCHO)	$CO_2 + 4H^+ + 4e^- \longrightarrow HCHO + H_2O$	-0.07
Carbon monoxide (CO)	$CO_2 + 2H^+ + 2e^- \longrightarrow CO + H_2O$	-0.10
Formic acid (HCOOH)	$CO_2 + 2H^+ + 2e^- \longrightarrow HCOOH$	-0.20
Methanol (CH_3OH)	$CO_2 + 6H^+ + 6e^- \longrightarrow CH_3OH + H_2O$	0.02
Ethanol (CH_3CH_2OH)	$2CO_2 + 12H^+ + 12e^- \longrightarrow CH_3CH_2OH + 3H_2O$	0.09

Useful parameters in ERC

To evaluate and compared the activity of electrocatalyst, there are some parameters which needs to clarify.

a) Onset potential: It is defined as the voltage applied on electrocatalyst versus reference electrode, under which the desired product is yielded at a detectable amount. It is always less than the equilibrium potential of CO_2 reduction and coming difference between them is referred as overpotential.

b) Faradaic efficiency (FE): It is the % age of electrons consumed for the formation of given product[9]. It can be calculated as:

$$\varepsilon_{Faradaic} = \alpha nF/Q$$

where Q is the total charge passed, F is the Faraday's constant, n is the number of moles and α is amount of electrons passed.

c) Overpotential (η): It is defined as the difference between actual electrode potential E and the equilibrium potential E_{eq}. The degree of polarization of an electrode in electrolytic cell is measured by overpotential.

$$\eta = E - E_{eq}$$

1.4.1 Electrochemical reduction of carbon dioxide

The research in ERC is increasingly growing. No doubt, ERC has huge benefits, but one has to deal with various challenges because of the simultaneous reactions, stable nature of CO_2, fast deactivation of electrocatalysts, low product selectivity.

The activation of this stable CO_2 molecule is necessary and first step required in the electrochemical reduction. In its structure, carbon forms double covalent bonds with oxygen and electron pairs are shared between them. CO_2 possess very high bond strength because of its *sp* hybridized linear structure[12]. Therefore, CO_2 needs substantial electrical potential to get activated. For CO_2 activation, the change in its geometry i.e. from linear to bent $\bullet CO_2^-$ (anion radical) required, leads to very slow self-exchange rate for the $CO_2/\bullet CO_2^-$, thus making this rate determining step. It requires -1.9V *vs.* SHE theoretically and considered as energy demanding step in the ERC. Therefore, there is a need of efficient electrocatalysts to lessen the activation barrier of energy. Due to similar reduction potentials of CO_2 and H_2 in electrochemical environment, SHE (simultaneous hydrogen evolution) reaction occurs at cathode. This leads to significant utilization of supplied energy for hydrogen evolution reaction rather getting used up in the CO_2 electroreduction due to competition between CO_2 electroreduction and hydrogen evolution reaction (HER) during ERC. Ultimately the current efficiency of the CO_2 electroreduction process is adversely affected. Thus, to make the

reaction selective towards ERC electrocatalysts are required and receives the most attention amongst all other challenges.

1.5 Electrocatalysts

According to IUPAC (1976), a catalyst being present in small proportions, increases the rate of reaction of chemical equilibrium without itself undergoing chemical change. The same thing is done by electrocatalyst but with electron transfer. It accelerates the variation in rate of reaction and contributes in electron transfer reaction at electrode. In electrochemistry, as in catalysis, rate of reaction depends only on given parameters but in case of electrocatalyst it depends on the electrode potential also. In electrochemical reactions, catalyst surface is in contact with other species (electrolyte ions and solvent molecules) also other than the reacting species which makes the electrocatalyst activity interesting. The two major types of catalysts used in electrochemical reduction are – Homogeneous catalyst and heterogeneous catalysts. There is a dispersion of catalyst particles in bulk in case of homogeneous catalyst while on the electrode surface the catalyst particles are coated in heterogeneous catalysts which makes both of them different from each other.

1.5.1 Homogeneous Electrocatalyst

Homogeneous electrocatalysts which participates in electrochemical reduction of CO_2 at cathode is transition metal complexes and gives reaction products. As discussed above, they are dispersed in bulk electrolyte. The major hindrance is the inertness of CO_2 molecule. Its coordination with transition metals is a favorable way to activate it. Due to this coordination, activation energy lowers required for further reactions and also enhances rate of reaction. Many reports of homogeneous electrocatalysts for electrochemical reduction have appeared in literature in past years. It produced reduction product of 2 electrons mostly i.e. CO^- and $HCOO^-$. The efficiency reaches up to 80 %. So, the homogeneous electrocatalysts considered as good for conversion of carbon dioxide into some other products.

1.5.2 Heterogeneous Electrocatalyst

Heterogeneous electrocatalysts leads to variety of products including alcohols, hydrocarbons, formic acid, carbon monoxide etc. In 2001, Sanchez *et. al* examined the reduction of carbon dioxide using copper electrodes to hydrocarbons. In their review, they

revealed that product formation depends on the conditions in which reaction has been carried out. The metal electrodes used in this process were divided on the basis of reaction product:-

(a) Copper for hydrocarbons and alcohols.

(b) Au, Ag, Zn, Ga for carbon monoxide.

(c) Pb, Hg, Sn for formic acid.

Heterogeneous electrocatalyst serves dual purpose in electrochemical reduction of CO_2 i.e. conversion and production of fuel. Various metal oxides coated on electrode surface are also used as heterogeneous electrocatalyst.

1.6 The objectives of thesis

The overall objective of the project is to develop electrocatalyst for the conversion of CO_2. The specific objectives are:

- Synthesis of support (graphene oxide) for the electrocatalyst
- Characterization of synthesized support for its relevant properties
- Synthesis and doping of bimetallic metal oxide on the support
- Characterization of bimetallic metal oxide electrocatalyst with various characterization techniques such as XRD, XPS. FE-SEM and Raman spectroscopy

1.7 Thesis overview

The purpose of this thesis is to deal with two major issues of the present world- the depletion of conventional fossil fuels and the rise in atmospheric temperature due to CO_2 emission. The use of CO_2 as a fuel is considered as appropriate solution of these problems. This thesis has been divided into five chapters.

Chapter 1 is introduction which covers background, basic knowledge about the current situation of atmospheric temperature. Various approaches to diminish CO_2 emissions, the details of the process of electrochemical reduction of carbon dioxide have been discussed in this chapter.

Chapter 2 discusses the literature review on the present status of electrochemical reduction of CO_2 and the use of various electrocatalysts. Thorough literature survey gives the idea about advantages and overcomes of already reported electrocatalysts.

Chapter 3 covers the materials used and the experimental methods that were carried out to synthesize the desired electrocatalyst. The different types of characterization techniques are also presented in this chapter.

Chapter 4 discusses the detailed study of sample with the help of various characterization techniques such as XRD, XPS, FE-SEM and Raman spectroscopy. The results of these techniques were also compared with literature to determine whether the synthesized electrocatalyst fulfill the desired requirement or not.

Chapter 5 is the summarized data of the work done and further recommendations of its future work.

CHAPTER 2 - LITERATURE REVIEW

Development of suitable electrocatalyst is inevitable and in previous years, many researchers have contributed their work towards it. Various categories such as metals, metal oxides, metal complexes and metal supported electrocatalysts have been used. Therefore, this study of literature has been carried out to know the efforts already made in this direction. This chapter provides the detailed literature survey on the recent developments made in electrocatalysts for electrochemical reduction of CO_2.

Yoshi Hori *et. al* [13] revealed the formation of various hydrocarbons at copper electrode in aqueous inorganic salt solution. They have determined the formation of CO and $HCOO^-$ at less negative potential and hydrocarbons at more negative potentials. As results, they concluded that the faradaic efficiencies of ethanol, propanol was 6.9 and 3.0 % at current density of 5 mA / cm^2 in $KHCO_3$ electrolyte. Michael Schwartz *et. al* [14] investigated electrocatalyst of perovskite-type merge with gas diffusion electrodes which stimulate CO_2 reduction to alcohols. Copper in Cu^{n+} state acts active and non-copper acts inactive towards this process. $La_{1.8}Sr_{0.2}CuO_4$ containing Teflon bonded carbon gas diffusion electrode exhibited the faradaic efficiency of 2.0, 30.5, 10% resp. for methanol, ethanol, n-propanol at 180 mA/cm^2. They also examine that by replacing Sr with Th in $La_{1.8}Sr_{0.2}CuO_4$, the overall action of catalyst decreased. Kohjiro Hara *et. al* [15] examined effect of charged passed, current density and CO_2 pressure on electrochemical reduction by increasing pressure on GDE having Pt electrocatalyst. They investigated that by increasing pressure product selectivities were also changed. They have examined the CO formation at low negative potential (-1.5 V) and methane, ethylene and ethanol at high negative potential (-1.7 V). As results, they succeeded in the formation of methane and ethanol at partial current densities of 313 and 19.8 mA/ cm^2 respectively.

Matthew W. Kanan *et. al* [16] investigated that by the reduction of thick Cu_2O films, CO_2 reduction over Cu electrodes occurred on low overpotential. They examined the formation of CO and HCO_2H at exceptional overpotential with high faradaic efficiencies. As results, they succeeded in the formation of CO and HCO_2H with faradaic efficiency of 45 % and 33 % at -0.3 to -0.5 V and -0.45 to -0.65 V respectively on annealed Cu whereas polycrystalline Cu shows faradaic efficiency of 20 % for CO at -0.8 V. Yihong Chen *et. al* [17] examined the aqueous CO_2 reduction on oxide-derived Au nanoparticles. They found that these electrodes presented the faradaic efficiency of 96 % for CO with current density of 2 - 4 mA / cm^2 at -

0.35 V and FE of 65 % at - 0.25 V having current density of 0.3 – 0.5 mA / cm^2. Whereas, polycrystalline Au shown very low current density and the decreases in FE of CO from 1-4 %. Jia-Xing Lu *et. al* [18] familiarized a highly efficient catalyst i.e. organically doped Palladium by framing pyridine derivative within metallic palladium for electroreduction of CO_2 to methanol. They found that pyridine ring is proven to be the key for the formation of methanol. The production of methanol with F.E. of 35 % at -0.6 V and formic acid is identified as major side product of reduction. They also revealed that irrespective of metal oxide cathode such as Cu_2O and Cu_2O/Zn electrode, their electrode has great advantage of stability and reusability.

L. M. Aeshala *et. al* [19] performed the reduction of carbon dioxide using cationic and anionic solid polymer electrolytes. They examined that faradaic efficiencies of products in presence of cationic electrolyte is less as compared to anionic electrolyte. For CH_4, C_2H_4 and CH_3OH maximum faradaic efficiency achieved was 32, 15 and 19 % respectively with the use of anionic solid polymer electrolyte. Dinghui Chi *et. al* [20] synthesized CuO nanoparticles of different morphology and utilized them for the electrochemical reduction of CO_2. As results, they concluded that ethanol, methanol propanol were formed but the amount of ethanol was more than 95 % at -1.7 V having current density of 10 mA / cm^2 which indicates the high selectivity of synthesized nanoparticles towards it. V. S. K. Yadav *et. al* [21] proposed the electrocatalytic activity of Sn and Co_3O_4 on electrochemical reduction of CO_2. As results, they detected that formic acid was the only product detected under all conditions. Maximum faradaic efficiency of 74.04 and 92.6 % were obtained at 1.5 and 2 V in $KHCO_3$ solution and 68.72 % were observed at 1.5 V in $NaHCO_3$.

Boon Siang Yeo *et. al* [22] shown the electrochemical reduction of CO_2 to C_2 compounds i.e. ethanol and ethylene on copper (I) oxide catalysts. They found that by changing the thickness of Cu_2O over layers the faradaic efficiencies of products were affected. They concluded that films of thickness 1.7-3.6 μm exhibited high selectivity and for ethylene F.E. of 34-39 % and for ethanol 9-16 % were achieved at current density of -30 mA / cm^2. V. S. K. Yadav *et. al* [23] in their work explained the electrocatalytic effect of cobalt oxide on cuprous oxide for the reduction of CO_2 electrochemically. They examined the formation of different products such as propanol, acetic acid, methanol, ethanol, formic acid and formaldehyde. Out of which, ethanol was the main product formed with high faradaic efficiency of 76.31 and 96.15 % at 1.5 and 2 V having current density of 0.9 and 4.5 mA / cm^2respectively. They also found that at 3 V, major products formed were ethanol with FE of 21.4 and propanol with FE of 30.2 % at reaction time of 5 minutes. Seunghwa Lee *et. al* [24] in their work represented the

electrocatalytic production of C_3-C_4 compounds on a Chloride-Induced Bi-Phasic Cu_2O-Cu Catalyst by transformation of CO_2. They examined the faradaic efficiency of 8.7 % for n-propanol and n- butane was also detected. Ethylene and ethanol were also produced with faradaic efficiency of 55 %.

Li Liu *et. al* [25] discussed the effect of modification of Ni, Zn, and Au of oxide derived copper electrode on CO_2 reduction. They compared the SEM images of different types of modifications and examined the rougher surface of oxide derived Cu then annealed Cu due to the formation of crystal domains. They also conclude that modification hardly changed the morphology of Cu electrode surface. They have examined that the modification by Ni increased the production of formic acid (1.6 %) and n-propanol (2.7 %) at -1.5 V which was higher than all modified electrodes. This is because it increases the production of CO and possess smaller radius thus results in lattice contraction. It also promotes coupling of C-C bonds. S. Ma *et. al* [26] represented the performance of Cu nanoparticles catalysts having different morphology and composition towards CO_2 reduction in alkaline electrolyzer. They found that catalyst morphology results in affecting product distribution. Use of GDEs with rougher surface of Cu catalysts leads to the achievement of high partial current densities i.e. -150 mA/cm^2 for ethylene and -48 mA/cm^2 for ethanol. The faradaic efficiencies for ethylene and ethanol were in range of 27- 46% and 7-17 % resp. A 10 fold raise in current density was achieved at low over potential of -0.58 V.

Dan Ren *et. al* [27] reported the sequences of oxide derived Cu_xZn catalysts for tuning the selectivity of electroreduction of CO_2 to ethanol. They found that by changing the quantity of Zn in Cu_xZn catalyst, the selectivity of production of ethanol *vs.* ethylene could be tuned by a factor of 12.5. On Cu_4Zn catalyst ethanol formation was exploited at -1.05 V having F.E. and partial current density of 29.1 % and -8.2 mA/ cm^2 respectively. Boon Siang Yeo *et. al* [28] investigated the stability of agglomerated Cu nanocrystals for the reduction process of CO_2 to propanol. They have found the exceptional catalytic activity of agglomerates of approx. 15 nm sized Cu Nanocrystals on electrochemical reaction. They also revealed that by doing simple modifications in structure of Cu catalyst one may achieve the notable efficiency in terms of stability, current density and onset potential. As results, they succeeded in the formation of n-propanol at -0.95 V on Cu nanocrystals with partial current density of -1.74 mA/ cm^2 which is remarkably 25 folds greater than that found on Cu^0 nanoparticles.

R.A. Geioushy *et. al* [29] in their work fabricated the electrocatalyst for reduction of CO_2 electrochemically to useful products at low over potential. As results, they concluded that GN/Cu_2O electrode shows high catalytic activity towards reduction at current density of 12.2

mA/ cm^2 at -1.7 V which is greater than Cu_2O electrode. They also revealed that ethanol was the leading product formed at -0.9 V having F.E. of 9.93 % and current density of 0.5257 mA/ cm^2. Jia-Xing Lu *et. al* [30] demonstrated a recyclable and highly stable doped alloy catalyst i.e. [PYD]@Cu–Pt which possess dual activity for electrochemical reduction of CO_2 and found that by just switching the potentials different alcohols were formed as products. They revealed the formation of pure methanol at -0.6 V and ethanol, propanol at -1.2 V with F.E. of 37 %, 24%, and 1% respectively having current density 22 mA/cm^2. They confirmed that the production of ethanol and propanol was due to the presence of copper component in catalyst.

Motiar Rahaman *et. al* [31] presented activated Cu Mesh as electrocatalyst for the reduction of CO_2 to multicarbon alcohols. It was found that electrodeposited Cu leads to formation of formate and ethylene with F.E. of 49.2 % at -0.7 V and 34.3 % at -1.1 V respectively and oxide derived Cu leads to production of propanol and ethanol having faradaic efficiencies of 13.1 and 13 % at -0.9 V and -1.0 V respectively. The partial current density reached to -1.33mA/cm^2 in case of propanol. Jing Yuan *et. al* [32] developed an active Cu supported on Titania catalyst for electroreduction of carbon dioxide into ethanol. They loaded the Cu NPs on TiO_2 surface by using it as a support and found the high catalytic activity towards electroreduction to ethanol. They used various wt. % ratio of Cu/TiO_2 catalyst and found that out of them 40 wt. % ratio showed 10 folded high faradaic efficiency for ethanol i.e. 27.4 % than Cu NPs i.e. 2.7 % at current density of 8.66 mA/ cm^2. R.A. Geioushy *et. al* [33] fabricated GN/ZnO/Cu_2O electrode with different weight ratios of ZnO/Cu_2O and used for CO_2 electro reduction in 0.5 M $NaHCO_3$ electrolyte. Linear sweep voltammetry shows increase in current density from 4mA/cm^2 to 8mA/cm^2 at -1.8 V. The maximum F.E. for propanol was 30% at -0.9 V vs. Ag/AgCl at weight ratio of 2:1.

Fengwang *et. al* [34] introduced a reduced graphene supported catalyst Sn/S_2 nanosheets which reduced CO_2 into $HCOO^-$ at overpotential of 0.23 V. The maximum product formed at 0.68 V and 13.9 mA cm^{-2} having F.E. of 84.5 %. With introducing sulfide derived catalyst, a new approach of class of catalyst comes into account for electroreduction of carbon dioxide. V. S. K. Yadav *et. al* [35] investigated the metal electrodes i.e. Sn and Zn coated on the surface of graphite plate for electroreduction. It was found that in comparison with Zn, Sn metal as electrocatalyst produced the maximum amount of product, with faradaic efficiency of 57.9% at 2 V in $KHCO_3$ solution as electrolyte. They also noticed that the only product at all voltages was HCOOH i.e. formic acid. Lu Chen *et. al* [36] performed the reduction of CO_2 in ionic liquid i.e. dimcarb (dimethylammonium dimethylcarbamate) using various metal

electrodes. Out of them, indium metal electrode shown better results and leads to the formation of $HCOO^-$ and CO having F.E. of 40 and 45 % respectively at -1.34 V.

V. S. K. Yadav *et. al* [37] performed the electrochemical reduction using Sn and Zn metal as electrocatalyst by coating them on the surface of graphite. The maximum faradaic efficiency of reduced product i.e. HCOOH was 45.33 % at 2.3 V in $KHCO_3$ solution. N. Gutierrez-Guerra *et. al* [38] used Cu based electrodes as catalyst on activated carbon, graphite and functionalized CNF as support. Out of them, Cu-G shows the production of alcohol i.e. methanol at -1.54 V having faradaic efficiency of 75 %. It was noticed that the selectivity of product varies with applied current (-10 mA to – 30 mA). Jeremy T. Feaster *et. al* [39] reported the activity of polycrystalline Sn as catalyst and found that $HCOO^-$as a reduced product of carbon dioxide, at -0.9 V, with the faradaic efficiency of 70 %.

Weixin Lv *et. al* [40] developed a bismuth based catalyst as a support on Cu foil. This electrodeposition catalyst reduced the CO_2 into formate in $KHCO_3$ solution. The selectivity of product was 91.3 % at 0.69 V. Chung Shou Chen *et. al* [41] found that copper mesocrystals remained active for many hours as compared to other copper based catalysts. The faradaic efficiency of ethylene was 27.2 % which is 18 times excess of methane at 0.99 V in $KHCO_3$. Heng Zhong *et. al* [42] studied the electrochemical reduction without bubbling CO_2 by using Cu electrode. It was done in 3 M $KHCO_3$ and many gaseous products such as CH_4, CO and C_2H_4 were formed but with low faradaic efficiency at prominent temperature. Table 2.1 and 2.2 shows the studies on the electroreduction of carbon dioxide using various metals and metal oxides during 1989-2017 respectively.

Table 2.1 Studies on electroreduction of carbon dioxide using metal electrocatalysts during 1989-2017

S. No.	Metal	Support/ Promoter	Working Electrode	Other electrodes		Electrolyte		Reaction condition(s)			Observations			Remark	References
				Anode	Reference electrode	Concen -tration	pH	Temp. /Pressure	V	CO_2 Flow rate (mL/min)	Product (FE %)	Current density (mA/cm^2)	Other		
1.	Cu	-	-	-	Ag/AgCl	0.45 M $KHCO_3$	-	25 °C	-	100	$HCOO^-$ (86)	22	-	-	43
2.	Ni	-	-	-	-	0.5 M $KHCO_3$	-	25 °C, 1atm	-	-	HCOOH (29), CO (1.7)	-	-	-	44
3.	Zn	-	-	-	-	MeOH+ NaOH+ Cu particles	-	-30 °C	-	-	HCOOH (7), CO (60), CH_4 (12)	-	-	-	45
4.	Cu mesh	-	-	-	-	0.45 M $KHCO_3$ + 1 M KCl	-	26 °C, 1.4 atm	-	-	$HCOO^-$ (86)	130	-	-	46
5.	Sn	-	-	-	-	0.5 M $KHCO_3$ + 2 M KCl	7.5	18 °C, 1 atm	-	-	$HCOO^-$ (91)	60	-	-	47
6.	Cu-Ni	-	-	-	-	$KHCO_3$ + MeOH (8:2)	-	-5 °C	-	-	HCOOH (13), CO (4), HCs (26)	-	-	-	48
7.	Pb	-	-	-	-	K_2HPO_4	7	25 °C, 1 atm	-	-	$HCOO^-$ (93)	-	-	-	49
8.	Pb	-	-	-	-	NaOH	8.5	21 °C	-	-	$HCOO^-$ (70)	2.5	-	-	50

9.	Cu	-	-	-	-	0.5 M K_2HPO_4	-	25 °C, 1 atm	-	-	HCOOH (6), CO (40), HCs (30)	-	-	-	51
10.	Cu mesh	-	-	-	-	$KHCO_3$	-	25 °C, 1 atm	-	-	CH_4 (19.4), C_2H_4 (18.7)	-	-	-	52
11.	In	-	-	-	-	$NaHCO_3$	8		-	-	$HCOO^-$ (45)	40	-	-	53
12.	Fe	-	-	-	-	0.5 M H_2SO_4	-	25 °C, 1 atm	-	-	CH_4, HCHO, C_2H_6, C_2H_5OH	-	-	-	54
13.	Pb	-	-	-	-	0.45 M $KHCO_3$ + HCl	-	25 °C, 1 atm	-	-	$HCOO^-$ (57)	10.5	-	-	55
14.	Bi/GC	-	-	-	-	CH_3CN	-	25 °C, 1 atm	-	-	CO (95)	-	-	-	56
15.	Sn/GDE	-	-	-	-	$NaHCO_3$	8.3	25 °C	1.6	-	$HCOO^-$ (70)	-	-	-	57
16.	Sn	-	-	-	-	$KHCO_3$	6.98	25 °C, 1 atm	-	-	$HCOO^-$ (91)	-	-	-	58
17.	Ag	-	-	-	-	BMImCl + 20 wt% H_2O	-	25 °C, 1 atm	-	-	CO (>99)	-	-	-	59
18.	Cu nanoc-ubes	-	-	-	-	0.1 M $KHCO_3$	-	-	0.60	-	C_2H_4	-	-	-	60

19.	Cu meso-crystals	-	-	-	-	0.1 M $KHCO_3$	-	-	0.99	-	CH_4 (1.5), C_2H_4 (27.2)	-	-	-	41
20.	Cu	-	-	-	-	0.1 M $KHCO_3$	-	-	-1.3	-	EtOH (6.9), Pr^nOH (3.0)	5	-	-	13
21.	GDE	-	-	-	-	0.5 M KOH	-	-	-2.6	-	EtOH(5), Pr^nOH (1),C_2H_4 (69), CH_4(9)	180	-	-	14
22.	GDE/ Pt	-	-	-	-	0.5 M $KHCO_3$	-	-	-1.7	-	EtOH (2.2), MeOH (35)	19.8	-	-	15
23.	Sn	-	-	-	-	0.5 M $KHCO_3$	-	-	2	-	HCOOH (92.6)	-	-	-	21
24.	Sn	Graphite plate	-	Co_3O_4	-	0.5 M $KHCO_3$	-	-	2	-	HCOOH (57.9)	-	-	-	35
25.	In	-	-	Pt foil	-	dimcarb	-	25 °C	1.34	-	$HCOO^-$ (40), CO (45)	-	-	-	36

26.	Zn	Graphite plate	-	Co_3O_4	-	0.5 M $KHCO_3$	-	-	2.3	-	HCOOH (45.33)	-	-	-	37
27.	Cu	Graphite	-	IrO_2	-	-	-	90	-1.54	-	MeOH (75)	-30	-	-	38
28.	Ag	Cu foil	-	Pt gauze	Ag/AgCl	0.5 M $KHCO_3$	-	RT	-1.7	-	CO (64.6)	-	-	-	61
29.	Bi	Cu foil	-	Pt	Ag/AgCl	0.1 M $KHCO_3$	-	-	-1.5	-	$HCOO^-$ (91.3)	-	-	-	40
30.	Sn	Oxide layer	-	-	Ag/AgCl	0.1 M $KHCO_3$	-	-	-1.8	-	$HCOO^-$ (84)	-	-	-	62
31.	Sn		-	-	Ag/AgCl	0.1 M $KHCO_3$	6.8	-	-0.9	-	HCOOH (70)	-	-	-	39
32.	Cu	Porous carbon	-	Pt/C	-	Amberlyst/SPEEK	-	-		-	HCOOH(0.7), CO (16)	3.3	-	-	63
33.	Sn/S_2	Reduced graphene oxide	Glassy carbon (3 mm)	Pt wire	Ag/AgCl	0.5 M $NaHCO_3$	-	22 °C	0.68	-	$HCOO^-$ (84.5)	13.9	-	-	34

Table 2.2 Studies on electroreduction of carbon dioxide using metal oxide electrocatalysts during 1989-2017

S. No.	Metal oxide	Support/ Promoter	Working electrode	Other electrodes		Electrolyte		Reaction condition(s)			Observations			Remark	References
				Anode	Reference electrode	Concen-tration	pH	Temp. /Pressure	V	CO_2 Flow rate (mL/min)	Product (FE %)	Current density (mA/cm^2)	Other		
1.	Cu_2O films	-	-	-	-	0.1 M $KHCO_3$	-	25 °C	-0.99	-	C_2H_4 (34-39) C_2H_5OH (9-16) CH_4	-	-	-	22
2.	Gd_2O_3 nanopart-icles	GC	-	-	-	0.1M TBAH/CH_3CN	-	25 °C, 1atm	-	-	CO	-	-	-	64
3.	CuO nanopart-icles	-	-	-	-	O.2 M KI	-	-	1.5	-	C_2H_5OH (35) C_3H_7OH (5)	-	-	-	20
4.	$Ir_{0.8}Ru_{0.2}$ oxide	Flat Ti Surface	-	-	-	0.4 M Briton Robinson buffer solution	5.8	4 and 22 °C, 1atm	-	-	C_2H_5OH (96 at 4^0 and 85 at $22^{°C}$)	-	-	-	65
5.	CuO (shell)	Cu (core)	-	-	-	1 M $KHCO_3$	-	25 °C, 1atm	-	-	CO(23) HCOOH (20) CH_3OH (1-3)	-	-	-	66
6.	γ-Ti_3O_5	-	-	-	-	-	-	-	1-2.5	-	CO (7), HCOOH (10)	-	-	-	67

7.	ZnO decorated with Cu nanoclusters	-	-	-	-	0.1 M $KHCO_3$	-	-	-1.20	-	CO (5.4), CH_4 (1.8), C_2H_4 (10), CH_3OH(2.8), C_2H_5OH (10), $HCOO^-$ (8)	-	-	-	68
8.	Cu from thick Cu_2O films	-	-	-	-	0.5 M $NaHCO_3$	-	-	Q≥ ~5 C· cm -2	-	CO (45), HCOOH (33), C_2H_4(5), C_2H_6 (10)	-	-	-	16
9.	Surface oxidized Cu	-	-	-	-	0.5 M KCl	-	25 °C	-	-	C_2H_6 (27)	-	-	-	69
10.	Electrodeposited Cu_2O	-	-	-	-	$KHCO_3$	7.6	25 °C	-	-	CH_3OH (38)	-	-	-	70
11.	Cu_2O	Zn disk	-	-	-	KOH/ methanol	7.5	-30 °C,	-	-	CH_4 (7.5), C_2H_4 (6.8)	-	-	-	71
12.	Cu_2O	Cu plate	-	-	-	$KHCO_3$	-	25 °C, 1 atm	-	-	C_2H_4 (22),	-	-	-	72

13.	RuO_2/ TiO_2 composites	Pt	-	-	-	0.5 M $NaHCO_3$	-	25 °C, 1 atm	-	-	CH_3OH (60.5)	-	-	-	73
14.	Cu_2O	Graphene	-	-	-	0.5 M $NaHCO_3$	-	-	-0.9	-	C_2H_5OH (9.93)	12.2	-	-	29
15.	Cu_2O/ ZnO	Graphene	-	-	-	0.5 M $NaHCO_3$	-	-	-0.9	-	C_3H_7OH (30)	12.2	-	-	33
16.	$Cu(OH)_2$	Cu nanowires	-	-	-	0.1 M $KHCO_3$	-	-	-1.1	-	C_2H_4 17.4	-	-	-	74
17.	SnO	ZnSe ATR-IR	Sn foil	Pt mesh	-	3 M NaCl	-	-	-1.4 - 1.8	-	H_2, $HCOO^-$,CO	-	-	-	75
18.	TiO_2	Cu	-	-	-	0.2 M KI	-	-	-1.45	-	C_2H_5OH (27.4)	8.66	-	-	32
19.	Cu_2O	-	-	-	-	0.1 M $KHCO_3$	-	-	-0.99	-	C_2H_4 (39), C_2H_5OH (9-16)	-	-	-	22
20.	Co_3O_4	Zn	-	-	-	0.5 M $KHCO_3$	-	-	1.5	-	HCOOH (78.5)	-	-	-	76
21.	Cu_2O	Carbon paper	-	-	-	PAA/PVA/KOH SPE	-	25 °C	3	20	CH_3OH, CH_4, CO	8.1	-	-	77

22.	MoS_x	PEI modified graphene	GCE	Pt wire	Ag/AgCl	0.5 M $NaHCO_3$	-	-	-0.65	-	CO (85.1)	-	-	-	78
23.	Cu_2O	Carbon paper	-	Pt/C	-	SPE	-	-	2.5	-	CH_3OH, CH_4	-	-	-	19
24.	Oxide derived Cu electrode	Ni, Zn, Au	Cu foil	Pt plate	-	0.1 M $NaHCO_3$	-	-	-1.2 to-1.6	-	HCOOH C_3H_7OH C_2H_5OH	-	-	-	25
25.	ZnO/ Al_2O_3	Cu	-	-	-	-	-	160 °C	-	30	C_2H_5OH	-	-	-	79
26.	Cu_2O	Cu disks	-	Pt wire	Ag/AgCl	0.1 M $KHCO_3$	-	-	-	20 sccm	C_2H_4 (42.6), C_2H_5OH (11.8), C_3H_7OH (5.4)	-13.3 -3.7 -1.7	-	-	80
27.	Cu_2O	Graphite plates	-	Co_3O_4	-	0.5M $KHCO_3$	-	-	2	-	C_2H_5OH (96.1) HCOOH	4.5	-	-	23
28	Cl induced bi phasic Cu_2O-Cu	-	Cu	Pt plate	Ag/AgCl	O.1 M KCl	-	-	-0.6 to -1.8	-	C_3H_7OH (8.7), C_4H_{10}, C_2H_4, C_2H_5OH	-	-	-	24

CHAPTER 3 - EXPERIMENTAL METHODS

The different materials have been used to prepare the electrocatalyst is mentioned in this chapter. The methods of synthesis of electrocatalyst along with their block diagrams and the specific characterization methods are also discussed.

3.1 Materials

Pure Graphite powder, sodium hydroxide pellets (98%), concentrated Sulphuric acid, sodium nitrate, sodium lauryl sulphate (99%), potassium permanganate, hydroxylamine hydrochloride (99%), hydrogen peroxide (30% concentration, w/v), cupric chloride, zinc chloride were purchased from LOBA Chemie Pvt. Ltd. Ethanol (99.9%, AR, Changshu Hongsheng Fine Chemicals). All the reagents and chemicals were of analytical grade and were used without any further purification.

3.2 Methods

3.2.1 Synthesis of Graphene Oxide (GO)

Hummer's method [81] was used to synthesized graphene oxide. In a 500 ml round bottom flask; graphite powder (2 g), 1 g of $NaNO_3$ (sodium nitrate) and 46 ml of conc. H_2SO_4 (sulfuric acid) were mixed and immersed in ice-water bath for strongly stirred of 15 minutes at 0 °C. Then, slowly addition of 6 g of $KMnO_4$ (potassium permanganate) to above solution was done and kept it too cooled down for 15 minutes. Potassium permanganate and sodium nitrate acts as catalysts and chemical reaction take place between graphene and concentrated sulphuric acid. The suspension solution was stirred continuously for 1 h and after that the slow addition of 92 ml of distilled water in the duration of 10 minutes into it. Subsequently, for the dilution of suspension solution 280 ml of warm water was added. The solution was treated with 10 ml of H_2O_2 (30%) to reduce the excess of $KMnO_4$. The resulting suspension was filtered followed by washing with water and kept in vacuum oven for 24 h at 60 °C for drying purpose. Figure 3.1 represents the block diagram of the synthesis of graphene oxide.

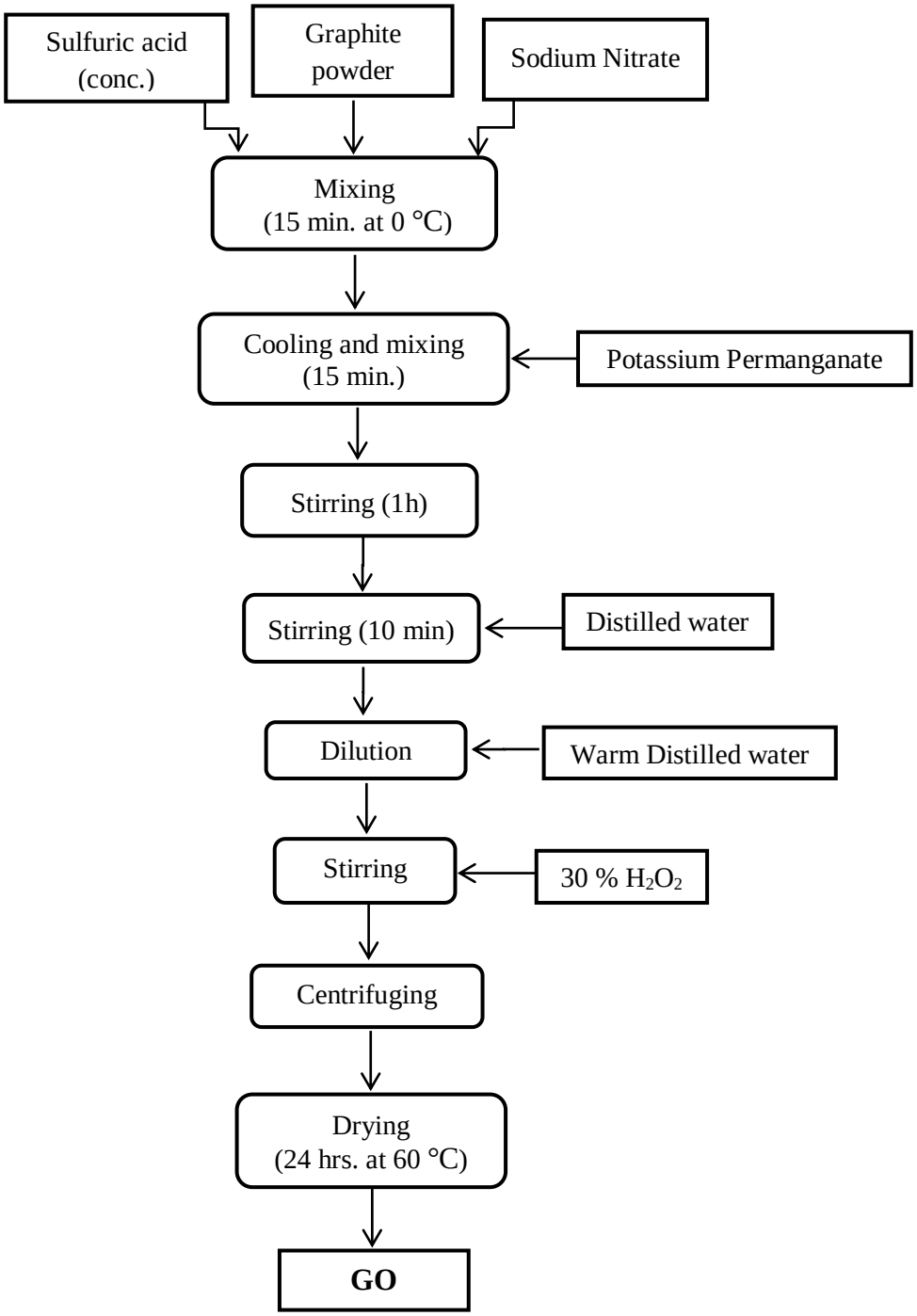

Fig 3.1 Block diagram of synthesis of graphene oxide

3.2.2 Synthesis of Cu_2O-ZnO/GN electrocatalyst

In a 500 ml round bottom flask, 6 ml of 6 mg ml^{-1} GO (graphene oxide) suspension solution was taken followed by addition of 366 ml ultrapure water into it and then sonicated it for 30 minutes. The calculated amounts i.e. 10.8 ml of 0.1 M $ZnCl_2$, 5.4 ml of 0.1 M $CuCl_2$ and 0.522 g SDS were added to above GO solution and kept for vigorous stirring at 34 °C for 2 h. Afterwards, 21.6 ml of 1.0 M NaOH (sodium hydroxide) and 96 ml of 0.1 M

$NH_2OH.HCl$ (hydroxylamine hydrochloride) were rapidly injected into above solution and stirred for another 30 minutes. The suspension solution was centrifuged and washed with water, followed by ethanol repeatedly. The obtained product was dried in vacuum oven for 18 h at 40 °C. Figure 3.2 represents the block diagram of synthesis of Cu_2O-ZnO/GN electrocatalyst.

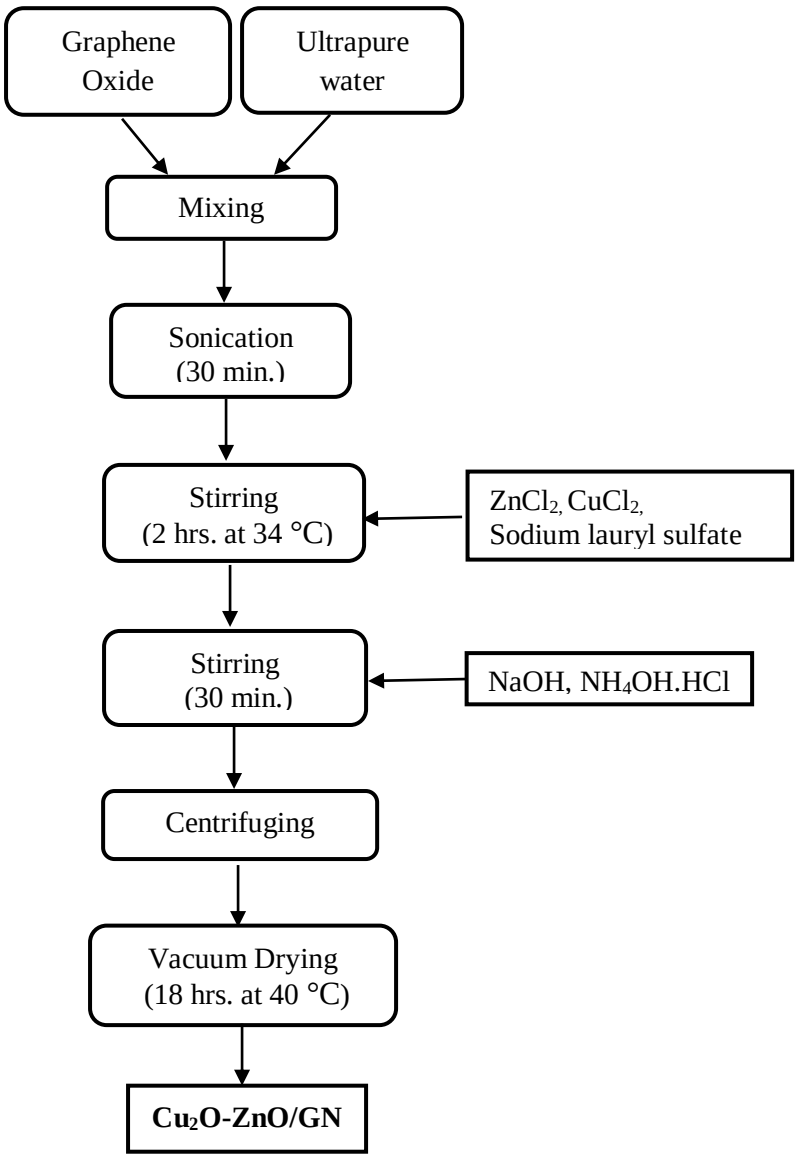

Fig 3.2 Block diagram of synthesis of Cu_2O-ZnO/GN electrocatalyst

3.3 Characterization methods

3.3.1 X-ray diffraction (XRD)

To determine the crystal structure of materials, XRD is one of the fast analytical methods being used. It can determine the phase identification of crystalline materials and gives the information about unit cell. The material should be finely ground, homogenized.

The constructive interference between X-Rays and electrons of sample materials results in the X-Ray diffraction. They are produced with the use of cathode tube and then filtered to get single beam radiation called monochromatic radiation. They are aligned parallel using collimator to make them concentrated before leading them to sample. For the constructive interference to produce it should satisfy the Bragg's law. PANalytical X'Pert PRO diffractometer was used to determine X-ray diffraction patterns of synthesized samples using Cu-K_α radiation. It was taken in 2θ range of 0- 10° and 10- 80° for low and wide angle respectively, with current and tube voltage of 40 mA and 45 kV.

3.3.2 Field emission scanning electron microscopy (FE-SEM)

This characterization technique is used to determine the surface morphologies of the synthesized sample. FE-SEM is more advanced form of SEM which provides energy beam of high quality and narrower nature. This provides better image quality ad resolution. This technique is able to done sample magnification higher than the range of 10Kx. JEOL JSM – 6510 LV, a field emission scanning electron microscope was used to analyzed the surface morphologies of samples at an accelerating voltage of 20 kV. To avoid sample charging issues, the sample was coated with gold of thickness 50 µm with the help of automatic sputter coater (Polaron).

3.3.3 X-ray photoelectron spectroscopy (XPS)

XPS measurements were carried out to identify oxygen, zinc and copper moieties on synthesized nanoparticles. It was carried on Kratos axis ultra DLD system using a monochromatic Al-Kα source operated at anode potential of 15 kV. The survey spectra were recorded with a pass energy of 50 eV while the high resolution spectra with a pass energy of 20 eV and emission current of 10 mA. The pressure of analysis chamber was maintained at 2×10^{-9} torr. XPS peak 4.1 software was used for data processing and the core level spectra were fitted with mixed Gaussian-Lorentzian convoluted function (80/20) and Shirley function was used for background substraction.

3.3.4 Raman spectroscopy

Raman spectroscopy is used to evaluate the structural changes occurs in the sample. It also examines the existence and position of disordered (D) and graphitic (G) bands and their intensity ratio. A confocal raman microscope (WITec alpha 300R, Germany) was used to obtained the raman spectra of synthesized samples having laser excitation of λ = 532 nm.

CHAPTER 4 - RESULTS AND DISCUSSIONS

The studies of prepared electrocatalyst using various spectroscopic techniques have been discussed in this chapter. The different techniques such as XPS, XRD, Raman spectroscopy and FE-SEM are analyzed in the following discussion.

4.1 X-ray Photoelectron Spectroscopy (XPS) analysis

The composition and valence state of elements are confirmed by XPS analysis. Figure 4.1 shows the fully scanned XPS spectrum in the range of 0-1100 eV. From these fully scanned spectra, only C, O, Cu and Zn elements were observed. Figure 4.2 (a) shows the high resolution spectra for C 1s region at 285 eV, which can be deconvoluted into three peaks. C 1s binding energy peaks at 283.8 eV, 284.8 eV and 288.4 eV were corresponds to C-C, C-O and C=O bands, respectively[82]. O 1s region at 530 eV high resolution spectra shown in figure 4.2 (b), after deconvolation into three different peaks at 531.4 eV, 530.4 eV and 529.7 eV which were attributed to C-O, OH and Zn-O bands, respectively. Figure 4.2 (c) shows that Zn 2p3/2 and Zn 2p1/2 which corresponds to 1021.5 eV and 1044.7 eV peaks respectively, confirms the Zn (II) oxidation state for ZnO. Also, figure 4.2 (d) shows that Cu 2P3/2 and Cu 2P1/2 which corresponds to 932.2 eV of Cu(I) oxidation state and 952 eV corresponds to Cu (II) oxidation state[29,33,82]. Table 4.1 shows the variation in C 1s, O 1s, Cu 2p and Zn 2p in binding energy, FWHM and area%.

Table 4.1 Variation in C 1s, O 1s, Cu 2p and Zn 2p in binding energy, FWHM and area%

Sample	Parameter	C1	C2	C3
Cu_2O-ZnO/GN	**BE (eV)**	283.8	284.8	288.6
	FWHM	0.92	2.11	4.13
	A%	21.33	49.12	29.54
		O1	**O2**	**O3**
	BE (eV)	529.6	530.4	531.6
	FWHM	0.99	1.14	1.47
	A%	33	46.24	20.75
		Cu 2P3/2	**Cu 2P1/2**	
	BE (eV)	932.2	952	
	FWHM	1.37	1.61	
	A%	68.90	31.09	
		Zn 2P3/2	**Zn 2P1/2**	
	BE (eV)	1021.5	1044.7	
	FWHM	1.47	1.67	
	A%	63.52	36.47	

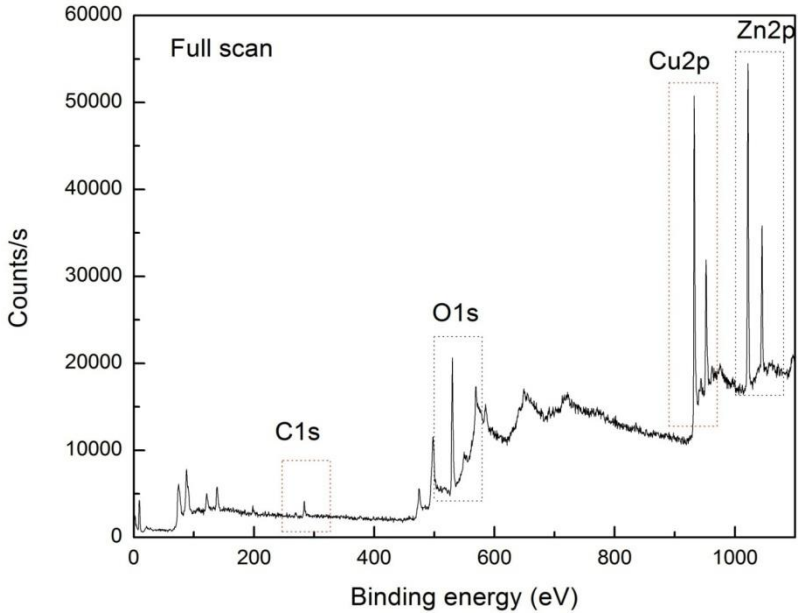

Fig. 4.1 Full scan XPS spectra for Cu_2O-ZnO/GN

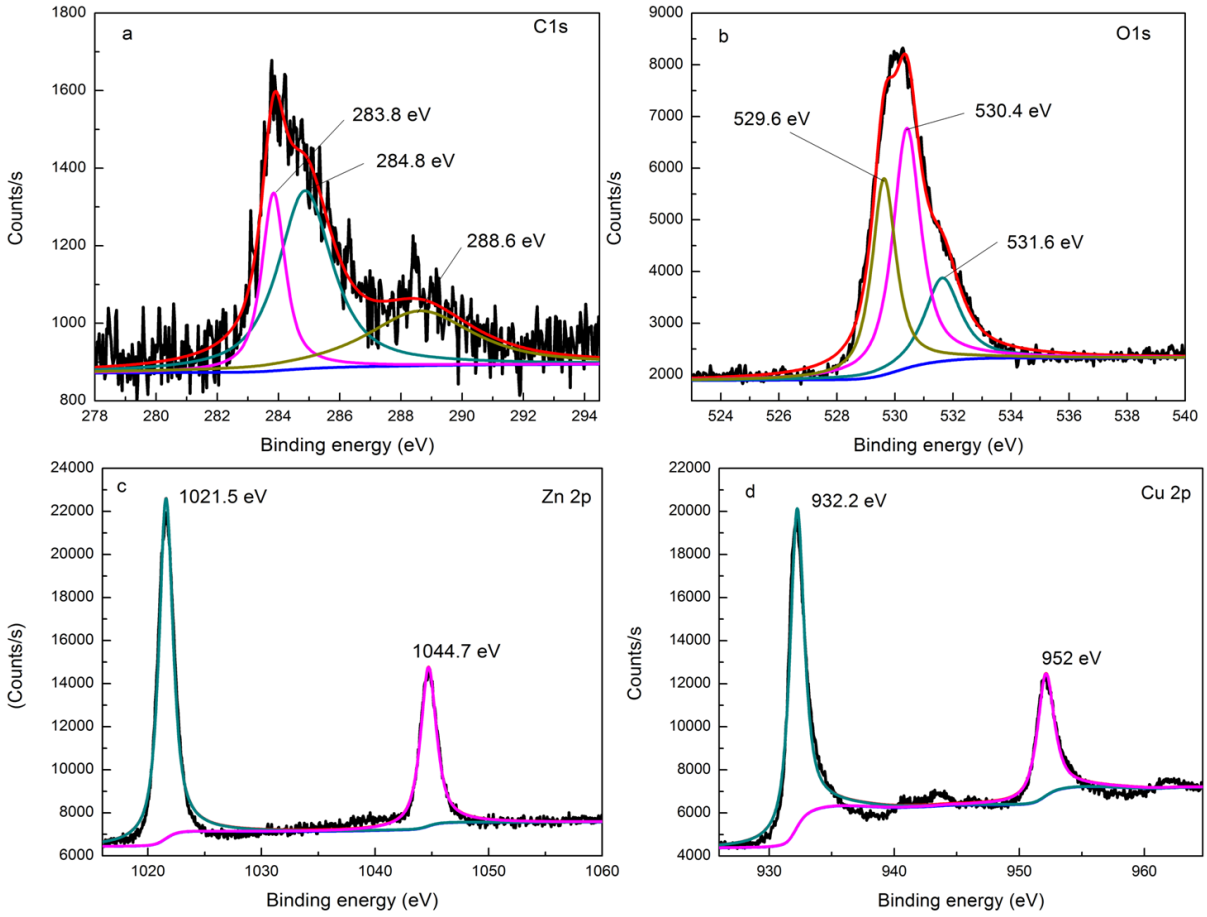

Fig. 4.2 XPS spectra for Cu_2O-ZnO/GN structure a) C 1s scan, b) O 1s scan, c) Zn 2P scan and d) Cu 2P scan

4.2 X-ray diffraction analysis

XRD analysis of as synthesized graphene oxide and Cu_2O-ZnO/GN electrocatalyst were carried out with the 2 theta values from 25-90° with the normal speed of 5°/min. As shown in figure 4.3, as synthesized graphene oxide shows broad diffraction peak at 25° and 43° which correspond to crystal orientations of (002) and (100) respectively[83]. XRD pattern for Cu_2O-ZnO/GN composite is shown in figure 4.4. The diffraction peaks at 31.91°, 34.65°, 47.93°, 56.81°, 63.05° and 68.19° corresponds to crystal orientations of (100), (002), (102), (110), (103), (112) planes of ZnO crystal structure respectively[33,82,84]. And the diffraction peaks at 28°, 38.75°, 40.97°, and 42.25° corresponds to crystal orientations of (110), (111), (200), (200) of Cu_2O crystal structure respectively[29,85-88]. A ZnO indicates highly crystalline structure as it shows sharp and narrow peaks. The crystallite size of nanoparticles are find out by using scherrers equation[89].

$$t = \frac{k.\lambda}{B.\cos\theta_B}$$

Where,

t= crystal thickness

k= constant representing shape factor (k is 0.89 for spherical, 0.94 for cubic and 0.9 for unknown size particle)

B= Full width at half maximum

θ_B= Bragg's angle

Crystallite size for Cu_2O crystal was found in the range of 10-50 nm and Crystallite size for ZnO crystal was found in the range of 21-48 nm as shown in table 4.2.

Table 4.2 Major peaks observed in XRD scan with D spacing, hkl index, FWHM and average crystallite size

2theta (degree)	Plane (hkl)	Crystal type	D spacing	FWHM (degree)	Crystallize Size (nm) (by Scherrer equation)
28	110	Cu_2O	3.1824	0.1771	48.30
31.91	100	ZnO	2.8019	0.2066	41.79
34.65	002	ZnO	2.5871	0.2362	36.81
36.47	101	ZnO	2.4614	0.2952	29.61
38.75	111	Cu_2O	2.3216	0.8266	10.65
40.97	200	Cu_2O	2.2008	0.2362	37.52
42.25	200	Cu_2O	2.138	0.1771	50.25
47.93	102	ZnO	1.8963	0.4133	21.98
56.81	110	ZnO	1.6192	0.4133	22.83
63.05	103	ZnO	1.4731	0.4133	23.56
68.19	112	ZnO	1.3742	0.3542	28.30

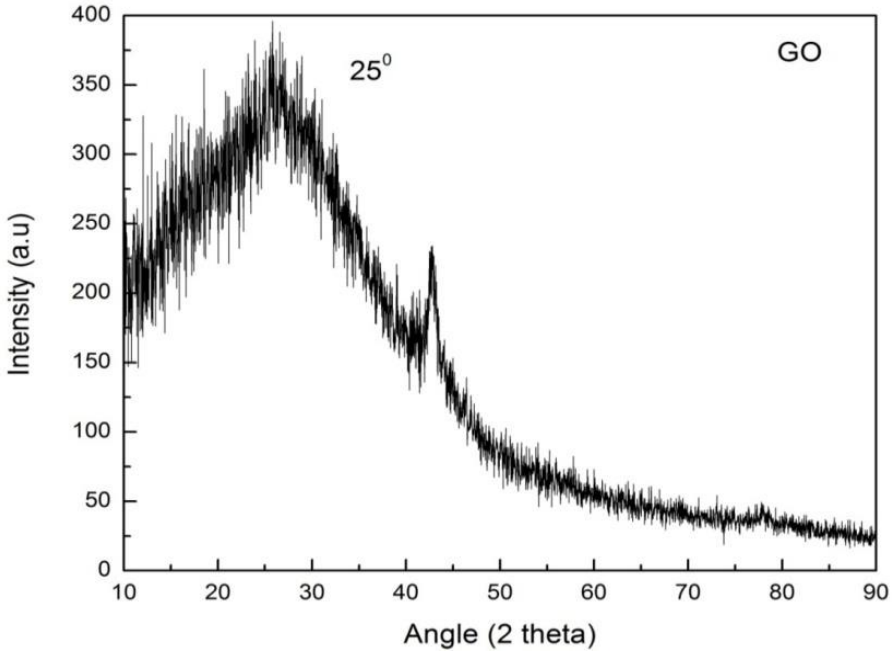

Fig. 4.3 XRD spectrum for graphene oxide by Hummer's method

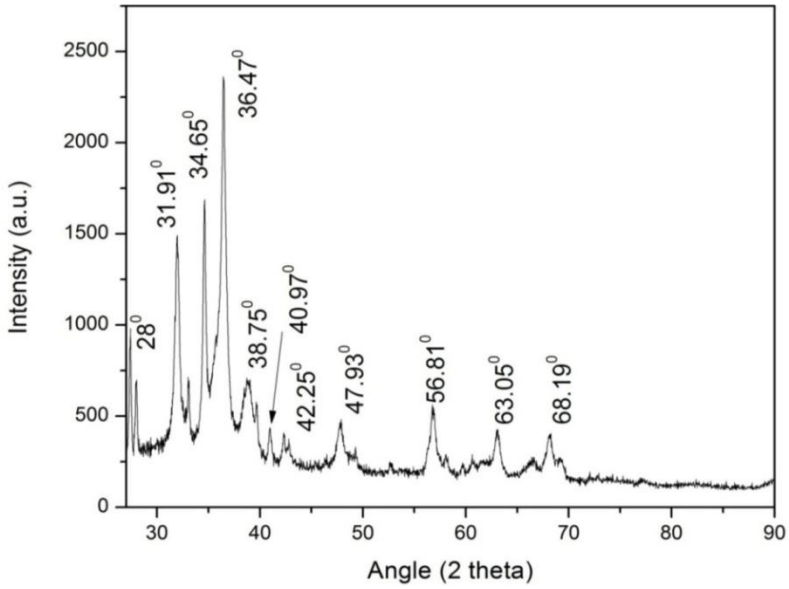

Fig. 4.4 XRD spectrum for as synthesized Cu_2O-ZnO/GN

4.3 Raman Spectroscopy

Order and disorder in carbon crystal structure is distinguished by Raman spectroscopy and it is powerful nondestructive technique. The typical Raman spectra for graphene oxide and Cu_2O-ZnO/GN are shown in figure 4.5. GO spectra shows D band and G band existence at 1350 and 1586 cm^{-1} [29,33]. The intensity ratio of D to G band (i.e. I_D/I_G) was observed for graphene oxide is 0.6551[83]. The intensity ratio of D/G band for Cu_2O-ZnO/GN should be higher than GO which confirms the removal of oxygen i.e. reduction of graphene oxide to graphene occurs[33]. But in synthesized sample, Cu_2O-ZnO/GN spectra shows the absence of D and G band, may be because of the layer of Cu_2O and ZnO is too thick on graphene material. So, the laser light could not reach to graphene and the energy was not absorbed.

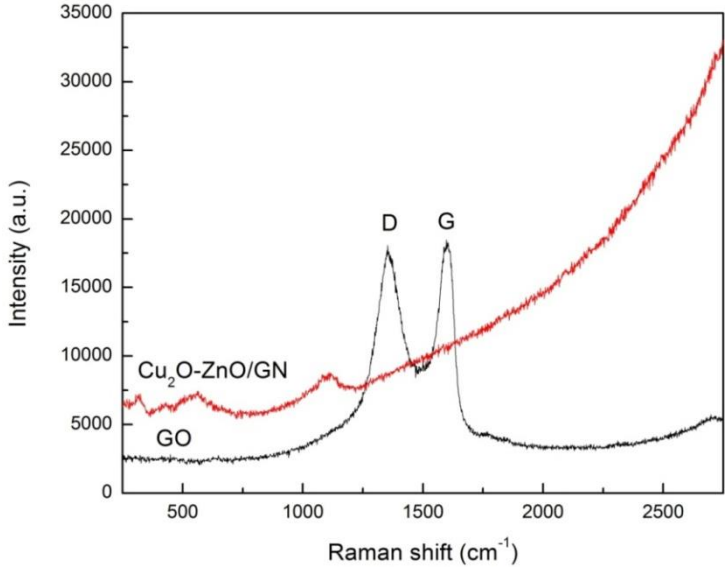

Fig. 4.5 Raman spectra for graphene oxide (GO) and Cu_2O-ZnO/GN

4.4 Field Emission Scanning Electron Microscopy (FESEM) analysis

The morphologies of as synthesized graphene oxide (GO) and Cu_2O-ZnO/GN electrocatalyst were characterized by FE-SEM as shown in figure 4.6. Here the surface morphologies of GO and Cu_2O-ZnO/GN are different. Graphene oxide shows the wrinkled layer morphology [83]. Also, it was observed that Cu_2O-ZnO deposited in the form of small particles on its surface. Cu_2O-ZnO shows the flower like morphology.

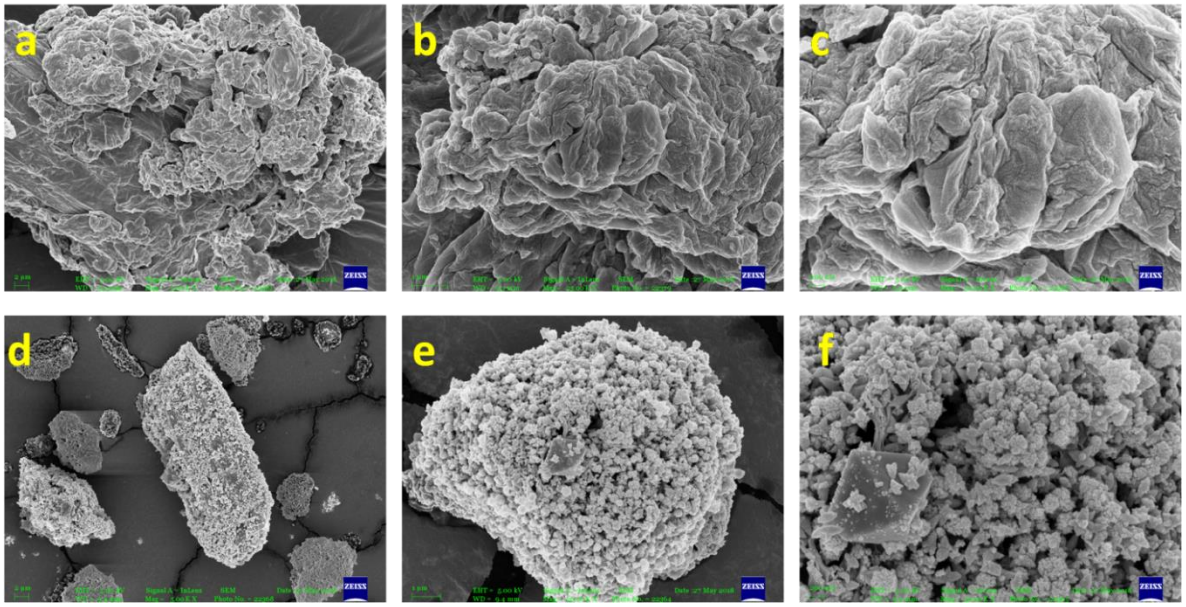

Fig. 4.6 FE-SEM images of Graphene oxide (a,b,c) and Cu_2O-ZnO/GN (d,e,f)

CHAPTER 5 - CONCLUSIONS AND RECOMMENDATIONS FOR FUTURE WORK

The overall results which have been analyzed in previous chapters are summarized and concluded in this chapter. The scope of future work has been discussed in this section.

5.1 Conclusions

In conclusion, graphene supported bimetallic metal oxide (Cu_2O-ZnO) electrocatalyst was synthesized using simple procedure at low temperature conditions. The graphene oxide was synthesized with the help of Hummer's method. The formation of electrocatalyst was confirmed with the results of characterization techniques such as XRD, XPS, FE-SEM and Raman spectroscopy.

The XRD pattern has shown the diffraction peaks at 31.91°, 34.65°, 47.93°, 56.81°, 63.05° and 68.19° which corresponds to crystal orientations of (100), (002), (102), (110), (103), (112) planes of ZnO crystal structure respectively and the diffraction peaks at 28°, 38.75°, 40.97°, and 42.25° corresponds to crystal orientations of (110), (111), (200), (200) of Cu_2O crystal structure respectively. A ZnO indicates highly crystalline structure as it shows sharp and narrow peaks. The morphology of prepared electrocatalyst was characterized by FE-SEM which indicates the wrinkled type and flower like morphology for graphene oxide and Cu_2O-ZnO respectively. The XPS analysis results confirmed the presence of oxygen, zinc and copper moieties on synthesized electrocatalyst. The Zn 2p3/2 and Zn 2p1/2 which corresponds to 1021.5 eV and 1044.7 eV peaks respectively, confirms the Zn (II) oxidation state for ZnO and Cu 2P3/2 and Cu 2P1/2 which corresponds to 932.2 eV of Cu (I) oxidation state and 952 eV corresponds to Cu (II) oxidation state respectively. In Raman spectroscopy, GO spectra shows D band and G band existence at 1350 and 1586 cm^{-1} respectively. The Cu_2O-ZnO/GN spectra shows the absence of D and G band, may be because of the layer of Cu_2O and ZnO is too thick on graphene material. So, the laser light could not reach to graphene and the energy was not absorbed. The results obtainable in this work show the potential and capability of Cu_2O-ZnO/GN as an electrocatalyst for electrochemical reduction of CO_2.

6.2 Recommendations for future work

From the results of characterization studies, it has been found that the prepared electrocatalyst is suitable for CO_2 reduction.

The following studies are recommended for the applications of prepared electrocatalyst:

- Further studies on the activity of prepared electrocatalyst in terms of selectivity of the desired products.
- The major hinder of CO_2 reduction is the durability of the electrocatalyst. Hence, estimation of the durability of electrocatalyst by further experimental studies is recommended.
- Figuring out the mechanism of the CO_2 reduction will help us to understand the interaction of electrocatalyst with CO_2 and hence with proper modification an electrocatalyst with high current density and low overpotential can be synthesized.

REFERENCES

(1) Hansen, J.; Sato, M.; Kharecha, P.; Beerling, D.; Berner, R.; Masson-Delmotte, V.; Pagani, M.; Raymo, M.; Royer, D. L.; Zachos, J. C. *arXiv preprint arXiv:0804.1126* **2008**.
(2) Yu, K. M. K.; Curcic, I.; Gabriel, J.; Tsang, S. C. E. *ChemSusChem* **2008**, *1*, 893.
(3) Plasynski, S.; Litynski, J.; McIlvried, H.; Srivastava, R. *Critical Reviews in Plant Science* **2009**, *28*, 123.
(4) Lal, R. *Critical Reviews in Plant Science* **2009**, *28*, 90.
(5) Markewitz, P.; Kuckshinrichs, W.; Leitner, W.; Linssen, J.; Zapp, P.; Bongartz, R.; Schreiber, A.; Müller, T. E. *Energy & environmental science* **2012**, *5*, 7281.
(6) Yusaf, T. F.; Noor, M. M.; Wandel, A. *Mild combustion: The future for lean and clean combustion*, 2013.
(7) Abbas, A.; Ullah, M.; Ali, Q.; Zahid, I.; Abbas, S.; Wang, X.; Taylor & Francis, ENGLAND: 2017.
(8) Tiwari, D.; Goel, C.; Bhunia, H.; Bajpai, P. K. *Separation and Purification Technology* **2017**, *181*, 107.
(9) Zhu, D. D.; Liu, J. L.; Qiao, S. Z. *Advanced Materials* **2016**, *28*, 3423.
(10) Meylan, F. D.; Moreau, V.; Erkman, S. *Journal of CO2 Utilization* **2015**, *12*, 101.
(11) Kortlever, R.; Shen, J.; Schouten, K. J. P.; Calle-Vallejo, F.; Koper, M. T. *The journal of physical chemistry letters* **2015**, *6*, 4073.
(12) Sullivan, B. P.; Krist, K.; Guard, H. *Electrochemical and electrocatalytic reactions of carbon dioxide*; Elsevier, 2012.
(13) Hori, Y.; Murata, A.; Takahashi, R. *Journal of the Chemical Society, Faraday Transactions 1: Physical Chemistry in Condensed Phases* **1989**, *85*, 2309.
(14) Schwartz, M.; Cook, R. L.; Kehoe, V. M.; MacDuff, R. C.; Patel, J.; Sammells, A. F. *Journal of the Electrochemical Society* **1993**, *140*, 614.
(15) Hara, K.; Kudo, A.; Sakata, T.; Watanabe, M. *Journal of the Electrochemical Society* **1995**, *142*, L57.
(16) Li, C. W.; Kanan, M. W. *Journal of the American Chemical Society* **2012**, *134*, 7231.
(17) Chen, Y.; Li, C. W.; Kanan, M. W. *Journal of the American Chemical Society* **2012**, *134*, 19969.
(18) Yang, H.-P.; Qin, S.; Wang, H.; Lu, J.-X. *Green Chemistry* **2015**, *17*, 5144.
(19) Aeshala, L.; Uppaluri, R.; Verma, A. *Journal of CO2 utilization* **2013**, *3*, 49.
(20) Chi, D.; Yang, H.; Du, Y.; Lv, T.; Sui, G.; Wang, H.; Lu, J. *RSC Advances* **2014**, *4*, 37329.
(21) Yadav, V.; Purkait, M. *RSC Advances* **2015**, *5*, 68551.
(22) Ren, D.; Deng, Y.; Handoko, A. D.; Chen, C. S.; Malkhandi, S.; Yeo, B. S. *ACS Catalysis* **2015**, *5*, 2814.
(23) Yadav, V.; Purkait, M. *Energy & Fuels* **2015**, *29*, 6670.
(24) Lee, S.; Kim, D.; Lee, J. *Angewandte Chemie* **2015**, *127*, 14914.
(25) Liu, L.; Tian, N.; Huang, L.; Hong, Y.-H.; Xie, A.-Y.; Zhang, F.-Y.; Xiao, C.; Zhou, Z.-Y.; Sun, S.-G. *Chinese Journal of Catalysis* **2016**, *37*, 1070.
(26) Ma, S.; Sadakiyo, M.; Luo, R.; Heima, M.; Yamauchi, M.; Kenis, P. J. *Journal of Power Sources* **2016**, *301*, 219.
(27) Ren, D.; Ang, B. S.-H.; Yeo, B. S. *ACS Catalysis* **2016**, *6*, 8239.
(28) Ren, D.; Wong, N. T.; Handoko, A. D.; Huang, Y.; Yeo, B. S. *The journal of physical chemistry letters* **2015**, *7*, 20.
(29) Geioushy, R.; Khaled, M. M.; Hakeem, A. S.; Alhooshani, K.; Basheer, C. *Journal of Electroanalytical Chemistry* **2017**, *785*, 138.
(30) Yang, H.-P.; Yue, Y.-N.; Qin, S.; Wang, H.; Lu, J.-X. *Green Chemistry* **2016**, *18*, 3216.

(31) Rahaman, M.; Dutta, A.; Zanetti, A.; Broekmann, P. *ACS Catalysis* **2017**, *7*, 7946.
(32) Yuan, J.; Liu, L.; Guo, R.-R.; Zeng, S.; Wang, H.; Lu, J.-X. *Catalysts* **2017**, *7*, 220.
(33) Geioushy, R.; Khaled, M. M.; Alhooshani, K.; Hakeem, A. S.; Rinaldi, A. *Electrochimica Acta* **2017**, *245*, 456.
(34) Li, F.; Chen, L.; Xue, M.; Williams, T.; Zhang, Y.; MacFarlane, D. R.; Zhang, J. *Nano Energy* **2017**, *31*, 270.
(35) Yadav, V.; Purkait, M. *RSC Advances* **2016**, *6*, 40916.
(36) Chen, L.; Guo, S. X.; Li, F.; Bentley, C.; Horne, M.; Bond, A. M.; Zhang, J. *ChemSusChem* **2016**, *9*, 1271.
(37) Yadav, V. S. K.; Purkait, M. K. *Energy & Fuels* **2016**, *30*, 3340.
(38) Gutiérrez-Guerra, N.; Moreno-López, L.; Serrano-Ruiz, J.; Valverde, J.; de Lucas-Consuegra, A. *Applied Catalysis B: Environmental* **2016**, *188*, 272.
(39) Feaster, J. T.; Shi, C.; Cave, E. R.; Hatsukade, T.; Abram, D. N.; Kuhl, K. P.; Hahn, C.; Nørskov, J. K.; Jaramillo, T. F. *ACS Catalysis* **2017**, *7*, 4822.
(40) Lv, W.; Zhou, J.; Bei, J.; Zhang, R.; Wang, L.; Xu, Q.; Wang, W. *Applied Surface Science* **2017**, *393*, 191.
(41) Chen, C. S.; Handoko, A. D.; Wan, J. H.; Ma, L.; Ren, D.; Yeo, B. S. *Catalysis Science & Technology* **2015**, *5*, 161.
(42) Zhong, H.; Fujii, K.; Nakano, Y. *Journal of Energy Chemistry* **2016**, *25*, 517.
(43) Hori, Y.; Konishi, H.; Futamura, T.; Murata, A.; Koga, O.; Sakurai, H.; Oguma, K. *Electrochimica acta* **2005**, *50*, 5354.
(44) SHUANG, S.; ZHIQIAO, H.; JIEXU, Y.; JIANMENG, C. *High technology letters* **2006**, *12*, 333.
(45) Kaneco, S.; Ueno, Y.; Katsumata, H.; Suzuki, T.; Ohta, K. *Chemical Engineering Journal* **2006**, *119*, 107.
(46) Li, H.; Oloman, C. *Journal of Applied Electrochemistry* **2006**, *36*, 1105.
(47) Li, H.; Oloman, C. *Journal of Applied Electrochemistry* **2007**, *37*, 1107.
(48) Satoshi, K.; Yuki, S.; Hideyuki, K.; Tohru, S.; Kiyohisa, O. *Bulletin of the Catalysis Society of India* **2007**, *6*, 74.
(49) Subramanian, K.; Asokan, K.; Jeevarathinam, D.; Chandrasekaran, M. *Journal of Applied Electrochemistry* **2007**, *37*, 255.
(50) Innocent, B.; Liaigre, D.; Pasquier, D.; Ropital, F.; Léger, J.-M.; Kokoh, K. *Journal of Applied Electrochemistry* **2009**, *39*, 227.
(51) Ikeda, S.; Ito, K.; Noda, H. In *AIP Conference Proceedings*; AIP: 2009; Vol. 1136, p 108.
(52) Goncalves, M.; Gomes, A.; Condeco, J.; Fernandes, R.; Pardal, T.; Sequeira, C.; Branco, J. *Energy Conversion and Management* **2010**, *51*, 30.
(53) Narayanan, S.; Haines, B.; Soler, J.; Valdez, T. *Journal of The Electrochemical Society* **2011**, *158*, A167.
(54) Pérez-Rodríguez, S.; García, G.; Calvillo, L.; Celorrio, V.; Pastor, E.; Lázaro, M. *International Journal of Electrochemistry* **2011**, *2011*.
(55) Alvarez-Guerra, M.; Quintanilla, S.; Irabien, A. *Chemical engineering journal* **2012**, *207*, 278.
(56) DiMeglio, J. L.; Rosenthal, J. *Journal of the American Chemical Society* **2013**, *135*, 8798.
(57) Prakash, G. S.; Viva, F. A.; Olah, G. A. *Journal of Power Sources* **2013**, *223*, 68.
(58) Lv, W.; Zhang, R.; Gao, P.; Lei, L. *Journal of Power Sources* **2014**, *253*, 276.
(59) Zhou, F.; Liu, S.; Yang, B.; Wang, P.; Alshammari, A. S.; Deng, Y. *Electrochemistry Communications* **2014**, *46*, 103.
(60) Roberts, F. S.; Kuhl, K. P.; Nilsson, A. *Angewandte Chemie* **2015**, *127*, 5268.

(61) Choi, J.; Kim, M. J.; Ahn, S. H.; Choi, I.; Jang, J. H.; Ham, Y. S.; Kim, J. J.; Kim, S.-K. *Chemical Engineering Journal* **2016**, *299*, 37.
(62) Zhang, R.; Lv, W.; Lei, L. *Applied Surface Science* **2015**, *356*, 24.
(63) Aeshala, L.; Rahman, S.; Verma, A. *Separation and purification technology* **2012**, *94*, 131.
(64) Behnamfar, M. T. *Journal of Particle Science & Technology* **2015**, *1*, 21.
(65) Ullah, N.; Ali, I.; Jansen, M.; Omanovic, S. *The Canadian Journal of Chemical Engineering* **2015**, *93*, 55.
(66) Lan, Y.; Gai, C.; Kenis, P. J.; Lu, J. *ChemElectroChem* **2014**, *1*, 1577.
(67) Sharma, P. P.; Ke, F.-S.; Zhou, X.-D. *ECS Transactions* **2014**, *61*, 331.
(68) Andrews, E.; Ren, M.; Wang, F.; Zhang, Z.; Sprunger, P.; Kurtz, R.; Flake, J. *Journal of The Electrochemical Society* **2013**, *160*, H841.
(69) Keerthiga, G.; Viswanathan, B.; Pulikottil, C. A.; Chetty, R. *Bonfring International Journal of Industrial Engineering and Management Science* **2012**, *2*, 41.
(70) Le, M.; Ren, M.; Zhang, Z.; Sprunger, P. T.; Kurtz, R. L.; Flake, J. C. *Journal of the Electrochemical Society* **2011**, *158*, E45.
(71) Ohya, S.; Kaneco, S.; Katsumata, H.; Suzuki, T.; Ohta, K. *Catalysis Today* **2009**, *148*, 329.
(72) Yano, J.; Yamasaki, S. *Journal of applied electrochemistry* **2008**, *38*, 1721.
(73) Qu, J.; Zhang, X.; Wang, Y.; Xie, C. *Electrochimica Acta* **2005**, *50*, 3576.
(74) Ma, M.; Djanashvili, K.; Smith, W. A. *Angewandte Chemie International Edition* **2016**, *55*, 6680.
(75) Baruch, M. F.; Pander III, J. E.; White, J. L.; Bocarsly, A. B. *ACS Catalysis* **2015**, *5*, 3148.
(76) Yadav, V. S. K.; Purkait, M. K. *New Journal of Chemistry* **2015**, *39*, 7348.
(77) Aeshala, L. M.; Verma, A. In *Macromolecular Symposia*; Wiley Online Library: 2015; Vol. 357, p 79.
(78) Li, F.; Zhao, S.-F.; Chen, L.; Khan, A.; MacFarlane, D. R.; Zhang, J. *Energy & Environmental Science* **2016**, *9*, 216.
(79) Zhao, B.; Liu, Y.; Zhu, Z.; Guo, H.; Ma, X. *Journal of CO2 Utilization* **2018**, *24*, 34.
(80) Handoko, A. D.; Ong, C. W.; Huang, Y.; Lee, Z. G.; Lin, L.; Panetti, G. B.; Yeo, B. S. *The Journal of Physical Chemistry C* **2016**, *120*, 20058.
(81) Wu, Z.-S.; Ren, W.; Gao, L.; Liu, B.; Jiang, C.; Cheng, H.-M. *Carbon* **2009**, *47*, 493.
(82) Luo, C.; Li, D.; Wu, W.; Yu, C.; Li, W.; Pan, C. *Applied Catalysis B: Environmental* **2015**, *166*, 217.
(83) Ji, Z.; Zhu, G.; Shen, X.; Zhou, H.; Wu, C.; Wang, M. *New Journal of Chemistry* **2012**, *36*, 1774.
(84) Ma, J.; Wang, K.; Li, L.; Zhang, T.; Kong, Y.; Komarneni, S. *Ceramics International* **2015**, *41*, 2050.
(85) Ha, H.-W.; Kim, I. Y.; Hwang, S.-J.; Ruoff, R. S. *Electrochemical and Solid-State Letters* **2011**, *14*, B70.
(86) Liu, Y.; Ma, L.; Zhang, D.; Han, G.; Chang, Y. *RSC Advances* **2017**, *7*, 12027.
(87) Lu, B.; Zhang, Z.; Hao, J.; Tang, J. *RSC Advances* **2014**, *4*, 21909.
(88) Zhang, S.; Liu, H.; Sun, C.; Liu, P.; Li, L.; Yang, Z.; Feng, X.; Huo, F.; Lu, X. *Journal of Materials Chemistry A* **2015**, *3*, 5294.
(89) Pike, J.; Chan, S.-W.; Zhang, F.; Wang, X.; Hanson, J. *Applied Catalysis A: General* **2006**, *303*, 273.

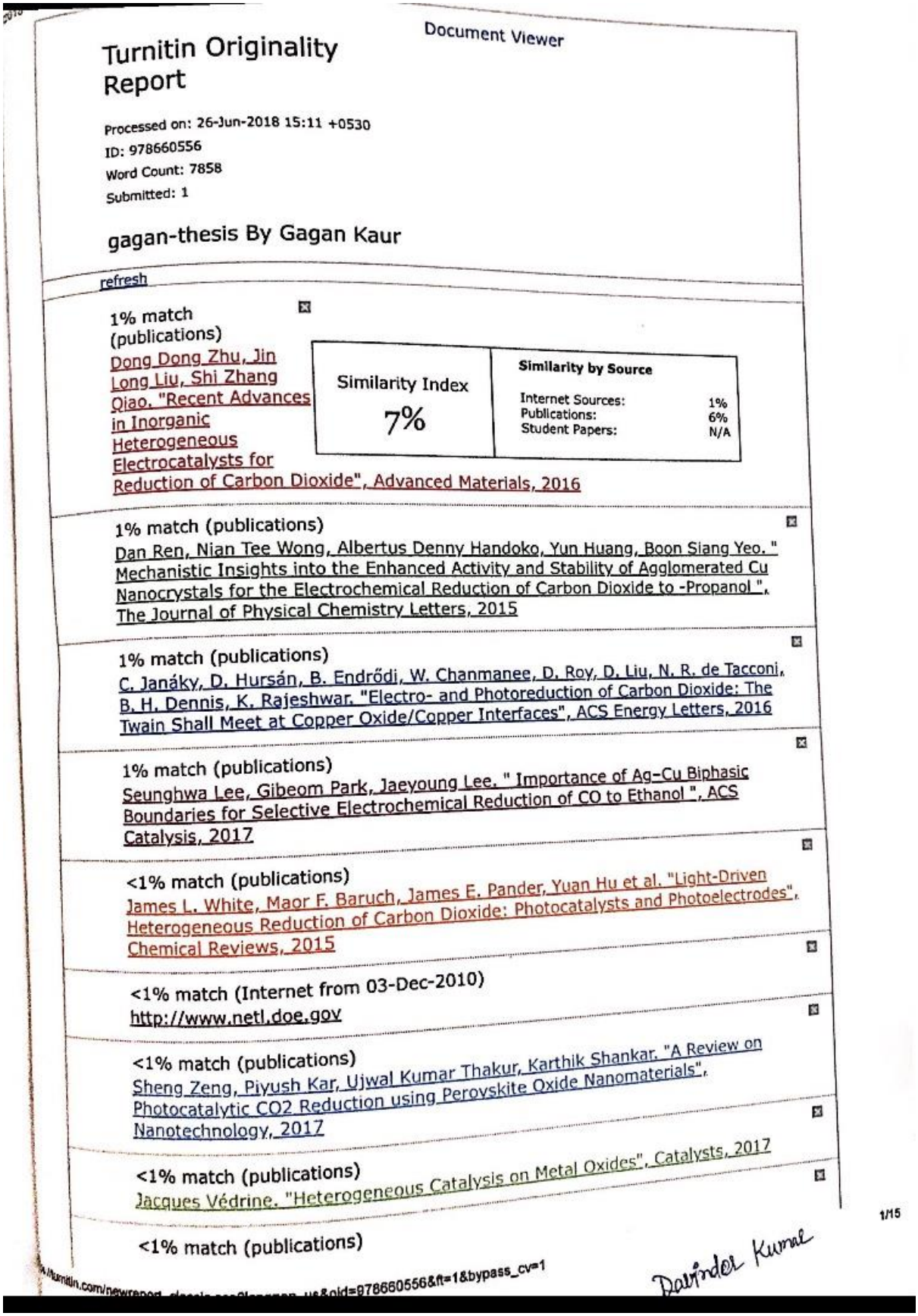

Turnitin Originality Report

Document Viewer

Processed on: 26-Jun-2018 15:11 +0530
ID: 978660556
Word Count: 7858
Submitted: 1

gagan-thesis By Gagan Kaur

refresh

Similarity Index	Similarity by Source	
7%	Internet Sources:	1%
	Publications:	6%
	Student Papers:	N/A

1% match (publications)
Dong Dong Zhu, Jin Long Liu, Shi Zhang Qiao, "Recent Advances in Inorganic Heterogeneous Electrocatalysts for Reduction of Carbon Dioxide", Advanced Materials, 2016

1% match (publications)
Dan Ren, Nian Tee Wong, Albertus Denny Handoko, Yun Huang, Boon Siang Yeo. " Mechanistic Insights into the Enhanced Activity and Stability of Agglomerated Cu Nanocrystals for the Electrochemical Reduction of Carbon Dioxide to -Propanol ", The Journal of Physical Chemistry Letters, 2015

1% match (publications)
C. Janáky, D. Hursán, B. Endrődi, W. Chanmanee, D. Roy, D. Liu, N. R. de Tacconi, B. H. Dennis, K. Rajeshwar, "Electro- and Photoreduction of Carbon Dioxide: The Twain Shall Meet at Copper Oxide/Copper Interfaces", ACS Energy Letters, 2016

1% match (publications)
Seunghwa Lee, Gibeom Park, Jaeyoung Lee, " Importance of Ag-Cu Biphasic Boundaries for Selective Electrochemical Reduction of CO to Ethanol ", ACS Catalysis, 2017

<1% match (publications)
James L. White, Maor F. Baruch, James E. Pander, Yuan Hu et al. "Light-Driven Heterogeneous Reduction of Carbon Dioxide: Photocatalysts and Photoelectrodes", Chemical Reviews, 2015

<1% match (Internet from 03-Dec-2010)
http://www.netl.doe.gov

<1% match (publications)
Sheng Zeng, Piyush Kar, Ujwal Kumar Thakur, Karthik Shankar, "A Review on Photocatalytic CO2 Reduction using Perovskite Oxide Nanomaterials", Nanotechnology, 2017

<1% match (publications)
Jacques Védrine, "Heterogeneous Catalysis on Metal Oxides", Catalysts, 2017

<1% match (publications)

1/15

Davinder Kumar